Neural Networks 131 (2020) 251–275

Contents lists available at ScienceDirect

Neural Networks

journal homepage: www.elsevier.com/locate/neunet

Review

Deep learning on image denoising: An overview

Chunwei Tian [a,b], Lunke Fei [c], Wenxian Zheng [d], Yong Xu [a,b,e,*], Wangmeng Zuo [f,e], Chia-Wen Lin [g]

[a] *Bio-Computing Research Center, Harbin Institute of Technology, Shenzhen, Shenzhen, 518055, Guangdong, China*
[b] *Shenzhen Key Laboratory of Visual Object Detection and Recognition, Shenzhen, 518055, Guangdong, China*
[c] *School of Computers, Guangdong University of Technology, Guangzhou, 510006, Guangdong, China*
[d] *Tsinghua Shenzhen International Graduate School, Shenzhen, 518055, Guangdong, China*
[e] *Peng Cheng Laboratory, Shenzhen, 518055, Guangdong, China*
[f] *School of Computer Science and Technology, Harbin Institute of Technology, Harbin, 150001, Heilongjiang, China*
[g] *Department of Electrical Engineering and the Institute of Communications Engineering, National Tsing Hua University, Hsinchu, Taiwan*

A R T I C L E I N F O

Article history:
Received 16 January 2020
Received in revised form 17 June 2020
Accepted 21 July 2020
Available online 6 August 2020

Keywords:
Deep learning
Image denoising
Real noisy images
Blind denoising
Hybrid noisy images

A B S T R A C T

Deep learning techniques have received much attention in the area of image denoising. However, there are substantial differences in the various types of deep learning methods dealing with image denoising. Specifically, discriminative learning based on deep learning can ably address the issue of Gaussian noise. Optimization models based on deep learning are effective in estimating the real noise. However, there has thus far been little related research to summarize the different deep learning techniques for image denoising. In this paper, we offer a comparative study of deep techniques in image denoising. We first classify the deep convolutional neural networks (CNNs) for additive white noisy images; the deep CNNs for real noisy images; the deep CNNs for blind denoising and the deep CNNs for hybrid noisy images, which represents the combination of noisy, blurred and low-resolution images. Then, we analyze the motivations and principles of the different types of deep learning methods. Next, we compare the state-of-the-art methods on public denoising datasets in terms of quantitative and qualitative analyses. Finally, we point out some potential challenges and directions of future research.
© 2020 Elsevier Ltd. All rights reserved.

Contents

* Corresponding author at: Bio-Computing Research Center, Harbin Institute of Technology, Shenzhen, Shenzhen, 518055, Guangdong, China.
E-mail address: yongxu@ymail.com (Y. Xu).

https://doi.org/10.1016/j.neunet.2020.07.025
0893-6080/© 2020 Elsevier Ltd. All rights reserved.

1. Introduction

Digital image devices have been widely applied in many fields, including recognition of individuals (Lei, Yuan, Wang, Wenhu, & Bo, 2016; Wen, Xu and Liu, 2020; Wen, Zhang, Zhang, Fei and Wang, 2020), and remote sensing (Du, Wei, & Liu, 2019). The captured image is a degraded image from the latent observation, in which the degradation processing is affected by factors such as lighting and noise corruption (Zha, Yuan, Yue, & Zhou, 2018; Zhang & Zuo, 2017). Specifically, the noise is generated in the processes of transmission and compression from the unknown latent observation (Xu, Zhang, & Zhang, 2018c). It is essential to use image denoising techniques to remove the noise and recover the latent observation from the given degraded image.

Image denoising techniques have attracted much attention in recent 50 years (Bernstein, 1987; Xu, Zhang, Zuo, Zhang and Feng, 2015). At the outset, nonlinear and non-adaptive filters were used for image applications (Huang, 1971). Nonlinear filters can preserve the edge information to suppress the noise, unlike linear filters (Pitas & Venetsanopoulos, 1986). Adaptive nonlinear filters depended on local signal-to-noise ratios to derive an appropriate weighting factor for removing noise from an image corrupted by the combination of additive random, signal-dependent, impulse noise and additive random noise (Bernstein, 1987). Non-adaptive filters can simultaneously use edge information and signal-to-noise ratio information to estimate the noise (Hong & Bao, 2000). In time, machine learning methods, such as sparse-based methods were successfully applied in image denoising (Dabov, Foi, Katkovnik, & Egiazarian, 2007). A non-locally centralized sparse representation (NCSR) method used nonlocal self-similarity to optimize the sparse method, and obtained high performance for image denoising (Dong, Zhang, Shi, & Li, 2012). To reduce computational costs, a dictionary learning method was used to quickly filter the noise (Elad & Aharon, 2006). To recover the detailed information of the latent clean image, priori knowledge (i.e., total variation regularization) can smooth the noisy image in order to deal with the corrupted image (Osher, Burger, Goldfarb, Xu, & Yin, 2005; Ren, Zuo, Zhang, Zhang and Yang, 2019). More competitive methods for image denoising can be found in Mairal, Bach, Ponce, Sapiro, and Zisserman (2009), Zuo, Zhang, Song, Zhang, and Gao (2014) and Zhang, Zuo, Chen, Meng and Zhang (2017), including the Markov random field (MRF) (Schmidt & Roth, 2014), the weighted nuclear norm minimization (WNNM) (Gu, Zhang, Zuo, & Feng, 2014), learned simultaneous sparse coding (LSSC) (Mairal et al., 2009), cascade of shrinkage fields (CSF) (Schmidt & Roth, 2014), trainable nonlinear reaction diffusion (TNRD) (Chen & Pock, 2016) and gradient histogram estimation and preservation (GHEP) (Zuo et al., 2014).

Although most of the above methods have achieved reasonably good performance in image denoising, they suffered from several drawbacks (Lucas, Iliadis, Molina, & Katsaggelos, 2018), including the need for optimization methods for the test phase, manual setting parameters, and a certain model for single denoising tasks. Recently, as architectures became more flexible, deep learning techniques gained the ability to overcome these drawbacks (Lucas et al., 2018).

The original deep learning technologies were first used in image processing in the 1980s (Fukushima & Miyake, 1982) and were first used in image denoising by Chiang and Sullivan (1989) and Zhou, Chellappa, and Jenkins (1987). That is, the proposed denoising work first used a neural network with both the known shift-invariant blur function and additive noise to recover the latent clean image. After that, the neural network used weighting factors to remove complex noise (Chiang & Sullivan, 1989). To reduce the high computational costs, a feedforward network was proposed to make a tradeoff between denoising efficiency and performance (Tamura, 1989). The feedforward network can smooth the given corrupted image by Kuwahara filters, which were similar to convolutions. In addition, this research proved that the mean squared error (MSE) acted as a loss function and was not unique to neural networks (Greenhill & Davies, 1994; de Ridder, Duin, Verbeek, & Van Vliet, 1999). Subsequently, more optimization algorithms were used to accelerate the convergence of the trained network and to promote the denoising performance (Bedini & Tonazzini, 1992; de Figueiredo & Leitao, 1992; Gardner, Wallace, & Stroud, 1989). The combination of maximum entropy and primal–dual Lagrangian multipliers to enhance the expressive ability of neural networks proved to be a good tool for image denoising (Bedini & Tonazzini, 1990). To further make a tradeoff between fast execution and denoising performance, greedy algorithms and asynchronous algorithms were applied in neural networks (Paik & Katsaggelos, 1992). Alternatively, designing a novel network architecture proved to be very competitive in eliminating the noise, through either increasing the depth or changing activation function (Sivakumar & Desai, 1993). Cellular neural networks (CENNs) mainly used nodes with templates to obtain the averaging function and effectively suppress the noise (Nossek & Roska, 1993; Sivakumar & Desai, 1993). Although this proposed method can obtain good denoising results, it requires the parameters of the templates to be set manually. To resolve this problem, the gradient descent was developed (Lee & de Gyvez, 1996; Zamparelli, 1997). To a certain degree, these deep techniques can improve denoising performance. However, these networks did not easily allow the addition of new plug-in units, which limited their applications in the real world (Fukushima, 1980).

Based on the reasons above, convolutional neural networks (CNNs) were proposed (Lo et al., 1995; Ren, Pan, Zhang, Cao and Yang, 2020). The CNN as well as the LeNet had real-world application in handwritten digit recognition (LeCun, Bottou, Bengio, Haffner, et al., 1998). However, due to the following drawbacks, they were not widely applied in computer systems (Krizhevsky, Sutskever, & Hinton, 2012). First, deep CNNs can generate vanishing gradients. Second, activation functions such as sigmoid (Marreiros, Daunizeau, Kiebel, & Friston, 2008) and tanh (Jarrett, Kavukcuoglu, Ranzato, & LeCun, 2009) resulted in high computational cost. Third, the hardware platform did not support the complex network. However, that changed in 2012 with AlexNet in that year's ImageNet Large-Scale Visual Recognition Challenge (ILSVRC) (Krizhevsky et al., 2012). After that, deep network architectures (e.g., VGG Simonyan & Zisserman, 2014 and GoogLeNet Szegedy et al., 2015) were widely applied in the fields of image (Li et al., 2020; Wang, Wang, Gao, Li, & Zuo, 2018; Wu & Xu,

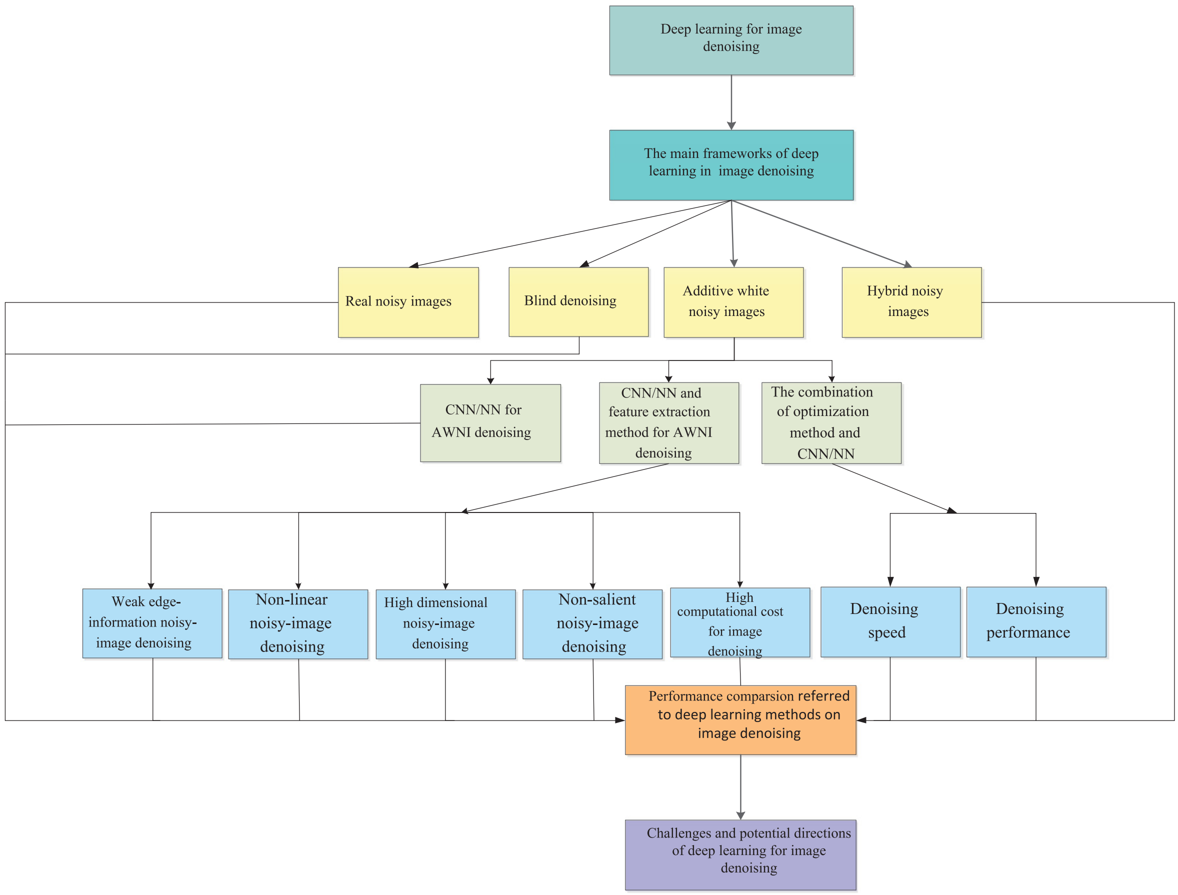

Fig. 1. Outline of the survey. It consists of four parts, including basic frameworks, categories, performance comparison, challenges and potential directions. Specifically, categories comprise additive white noisy images, real noisy images, blind denoising and hybrid noisy images.

2019), video (Liu, Lu, He, Zhang and Chen, 2017; Yuan, Li, He, Liu and Lu, 2020), nature language processing (Duan et al., 2018) and speech processing (Zhang et al., 2018), especially low-level computer vision (Peng et al., 2019; Tian et al., 2019).

Deep networks were first applied in image denoising in 2015 (Liang & Liu, 2015; Xu, Zhang and Zhang, 2015). The proposed network need not manually set parameters for removing the noise. After then, deep networks were widely applied in speech (Zhang et al., 2015), video (Yuan, Fan and He, 2020) and image restoration (Ren et al., 2020; Tian et al., 2020). Mao, Shen, and Yang (2016) used multiple convolutions and deconvolutions to suppress the noise and recover the high-resolution image. For addressing multiple low-level tasks via a model, a denoising CNN (DnCNN) (Zhang, Zuo, Chen et al., 2017) consisting of convolutions, batch normalization (BN) (Ioffe & Szegedy, 2015), rectified linear unit (ReLU) (Nair & Hinton, 2010) and residual learning (RL) (He, Zhang, Ren, & Sun, 2016) was proposed to deal with image denoising, super-resolution, and JPEG image deblocking. Taking into account the tradeoff between denoising performance and speed, a color non-local network (CNLNet) (Lefkimmiatis, 2017) combined non-local self-similarity (NLSS) and CNN to efficiently remove color-image noise.

In terms of blind denoising, a fast and flexible denoising CNN (FFDNet) (Zhang, Zuo, & Zhang, 2018a) presented different noise levels and the noisy image patch as the input of a denoising network to improve denoising speed and process blind denoising. For handling unpaired noisy images, a generative adversarial network (GAN) CNN blind denoiser (GCBD) (Chen, Chen, Chao and Yang, 2018) resolved this problem by first generating the ground truth, then inputting the obtained ground truth into the GAN to train the denoiser. Alternatively, a convolutional blind denoising network (CBDNet) (Guo, Yan, Zhang, Zuo, & Zhang, 2019) removed the noise from the given real noisy image by two sub-networks, one in charge of estimating the noise of the real noisy image, and the other for obtaining the latent clean image. For more complex corrupted images, a deep plug-and-play super-resolution (DPSR) method (Zhang, Zuo and Zhang, 2019) was developed to estimate blur kernel and noise, and recover a high-resolution image. Although other important research has been conducted in the field of image denoising in recent years, there have been only a few reviews to summarize the deep learning techniques in image denoising (Tian, Xu, Fei, & Yan, 2018). Although Ref. Tian et al. (2018) referred to a good deal work, it lacked more detailed classification information about deep learning for image denoising. For example, related work pretraining to unpaired real noisy images was not covered. To this end, we aim to provide an overview of deep learning for image denoising, in terms of both applications and analysis. Finally, we discuss the state-of-the-art methods for image denoising, including how they can be further expanded to respond to the challenges of the future, as well as potential research directions. An outline of this survey is shown in Fig. 1.

This overview covers more than 200 papers about deep learning for image denoising in recent years. The main contributions in this paper can be summarized as follows.

1. The overview illustrates the effects of deep learning methods on the field of image denoising.

2. The overview summarizes the solutions of deep learning techniques for different types of noise (i.e., additive white noise, blind noise, real noise and hybrid noise) and analyzes the motivations and principles of these methods in image denoising,

where blind noise denotes noise of unknown types. Finally, we evaluate the denoising performance of these methods in terms of quantitative and qualitative analyses.

3. The overview points out some potential challenges and directions for deep learning in the use of image denoising.

The rest of this overview is organized as follows.

Section 2 discusses the popular deep learning frameworks for image applications. Section 3 presents the main categories of deep learning in image denoising, as well as a comparison and analysis of these methods. Section 4 offers a performance comparison of these denoising methods. Section 5 discusses the remaining challenges and potential research directions. Section 6 offers the authors' conclusions.

2. Fundamental frameworks of deep learning methods for image denoising

This section offers a discussion of deep learning, including the ideas behind it, the main network frameworks (techniques), and the hardware and software, which is the basis of the deep learning techniques for image denoising covered in this survey.

2.1. Machine learning methods for image denoising

Machine learning methods consist of supervised, semi-supervised and unsupervised learning methods. Supervised learning methods (Li, Lu, Zhang, You and Zhang, 2019; Litjens et al., 2017; Xiao et al., 2019) use the given label to put the obtained features closer to the target for learning parameters and training the denoising model. For example, take a given denoising model $y = x + \mu$, where x, y and μ represent the given clean image, noisy image and additive Gaussian noise (AWGN) of standard deviation σ, respectively. From the equation above and Bayesian knowledge, it can be seen that the learning of parameters of the denoising model relies on pair $\{x_k, y_k\}_{k=1}^N$, where x_k and y_k denote the kth clean image and noisy image, respectively. Also, N is the number of noisy images. This processing can be expressed as $x_k = f(y_k, \theta, m)$, where θ is the parameters and m denotes the given noise level.

Unsupervised learning methods (Lee et al., 2018) use given training samples to find patterns rather than label matching and finish specific tasks, such as unpairing real low-resolution images (Yuan et al., 2018). The recently proposed Cycle-in-Cycle GAN (CinCGAN) recovered a high-resolution image by first estimating the high-resolution image as a label, then exploiting the obtained label and loss function to train the super-resolution model.

Semi-supervised learning methods (Choi, Vania, & Kim, 2019) apply a model from a given data distribution to build a learner for labeling unlabeled samples. This mechanism is favored by small sample tasks, such as medical diagnosis. A semi-supervised learned sinogram restoration network (SLSR-Net) can learn feature distribution from paired sinograms via a supervised network, and then, convert the obtained feature distribution to a high-fidelity sinogram from unlabeled low-dose sinograms via an unsupervised network (Meng et al., 2020).

2.2. Neural networks for image denoising

Neural networks are the basis of machine learning methods, which in turn are the basis of deep learning techniques (Schmidhuber, 2015). Most neural networks consist of neurons, input X, activation function f, weights $W = [W^0, W^1, \ldots, W^{n-1}]$ and biases $b = [b^0, b^1, \ldots, b^n]$. The activation functions such as sigmoid (Karlik & Olgac, 2011; Marreiros et al., 2008) and tanh (Fan, 2000; Jarrett et al., 2009) can convert the linear input into non-linearity through W and b as follows.

$$f(X; W; b) = f(W^T X + b). \tag{1}$$

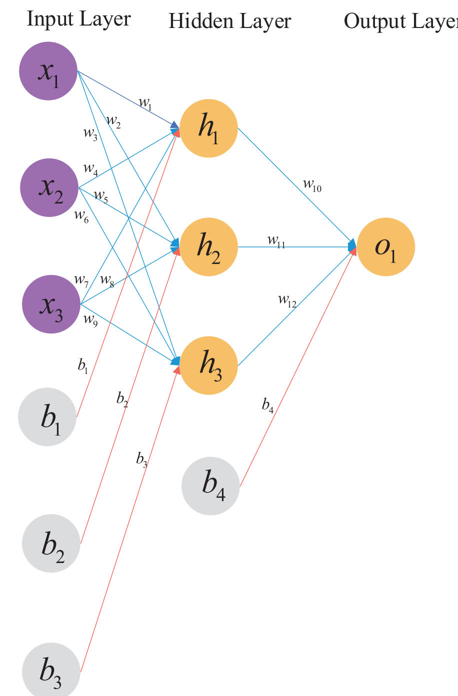

Fig. 2. Two-layer neural network.

Note that if the neural network has multiple layers, it is regarded as multilayer perceptron (MLP) (Burger, Schuler, & Harmeling, 2012). In addition, the middle layers are treated as hidden layers besides the input and output layers. This process can be expressed as

$$f(X; W; b) = f(W^n f(W^{n-1} \ldots f(W^0 X + b^0) \ldots b^{n-1}) + b^n), \tag{2}$$

where n is the final layer of the neural network. To help readers understand the principle of the neural network, a visual example is provided in Fig. 2.

The two-layer fully connected neural network includes two layers: a hidden layer and output layer (the input layer is not generally regarded as a layer of a neural network). There are parameters to be defined: x_1, x_2, x_3 and o_1 represent the inputs and output of this neural network, respectively. $w_1, w_2, \ldots, w_{11}, w_{12}$ and b_1, b_2, b_3, b_4 are the weights and biases, respectively. For example, the output of one neuron h_1 via Eqs. (3) and (4) is obtained as follows:

$$f(z_{h1}) = f(w_1 x_1 + w_4 x_2 + w_7 x_3 + b_1). \tag{3}$$

$$o(h_1) = f(z_{h1}). \tag{4}$$

First, the output of the network o_1 is obtained. Then, the network uses back propagation (BP) (Hirose, Yamashita, & Hijiya, 1991) and loss function to learn parameters. That is, when the loss value is within specified limitation, the trained model is considered as well-trained. It should be noted that if the number of layers of a neural network is more than three, it is also referred to as a deep neural network. Stacked auto-encoders (SARs) (Hinton & Salakhutdinov, 2006) and deep belief networks (DBNs) (Bengio, Lamblin, Popovici, & Larochelle, 2007; Hinton & Osindero, 2006) are typical deep neural networks. They used stacked layers in an unsupervised manner to train the models and obtain good performance. However, these networks are not simple to implement and require a good deal of manual settings to achieve an optimal model. Due to this, end-to-end connected networks, especially CNNs, were proposed (Yao, Wu, Zhang, Shan,

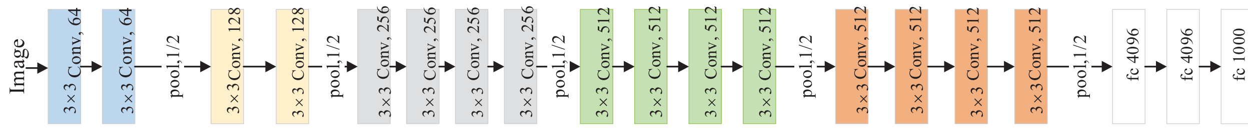

Fig. 3. Network architecture of VGG.

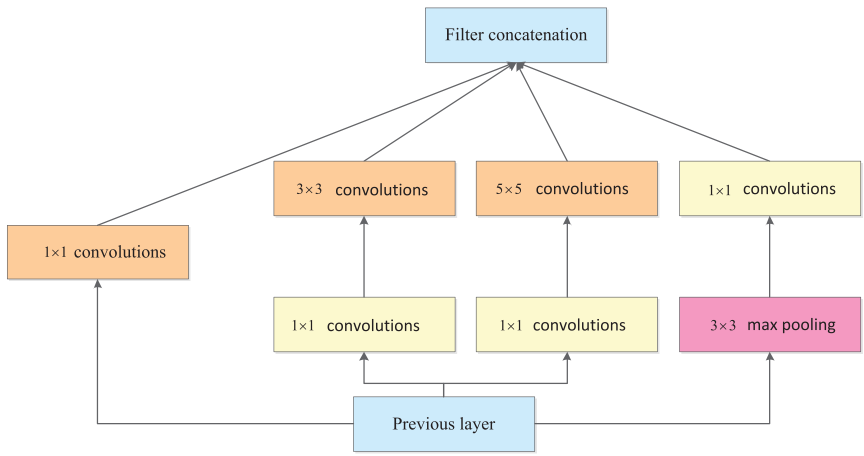

Fig. 4. Network architecture of GoogLeNet (Inception 1).

& Zuo, 2018). CNNs have wide applications in the field of image processing, especially image denoising.

2.3. CNNs for image processing

Due to their plug-and-play network architectures, CNNs have achieved great success in image processing (Li, Zhang, & Zhang, 2017; Lu et al., 2018; Zhang & Ghanem, 2018). As a pioneer in CNN technology, LeNet (LeCun et al., 1998) used convolutional kernels of different sizes to extract features and obtain good performance in image classification. However, due to the sigmoid activation function, LeNet had a slow convergence speed, which was a shortcoming in real-world applications.

After LeNet, the proposed AlexNet (Krizhevsky et al., 2012) was a milestone for deep learning. Its success was due to several reasons. First, the graphics processing unit (GPU) (Marreiros et al., 2008) provided strong computational ability. Second, random clipping (i.e., dropout) solved the overfitting problem. Third, ReLU (Nair & Hinton, 2010) improved the speed of stochastic gradient descent (SGD) rather than sigmoid (Bottou, 2010). Fourth, the data augmentation method further addressed the overfitting problem. Although AlexNet achieved good performance, it required substantial memory usage due to its large convolutional kernels. That limited its real-world applications, such as in smart cameras. After that, during the period of 2014 to 2016, deeper network architectures with small filters were preferred to improve the performance and reduce computational costs. Specifically, VGG (Simonyan & Zisserman, 2014) stacked more convolutions with small kernel sizes to win the ImageNet LSVR Challenge in 2014. Fig. 3 depicts the network architecture.

With the success of deeper networks, the research turned to increasing their width. GoogLeNet (Szegedy et al., 2015) increased the width to improve the performance for image applications. Moreover, GoogLeNet transformed a large convolutional kernel into two smaller convolution kernels in order to reduce the number of parameters and computational cost. GoogLeNet also used the inception module (Lin, Chen, & Yan, 2013) as well as Inception 1. Its visual network figure is shown in Fig. 4.

Although VGG and GoogLeNet methods are effective for image applications, they have two drawbacks: if the network is very deep, this may result in vanishing or exploding gradients; and if the network is very wide, it may be subject to the phenomenon of overfitting. To overcome these problems, ResNet (He et al., 2016) was proposed in 2016. Each block was given by adding residual learning operation in ResNet to improve the performance of image recognition, which leads to ResNet winning the mageNet LSVR in 2015. Fig. 5 depicts the concept of residual learning.

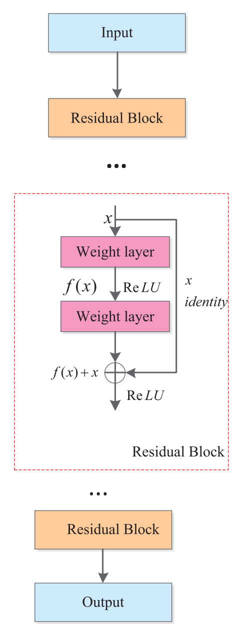

Fig. 5. Network architecture of ResNet.

Since 2014, deep networks have been widely used in real-world image applications, such as facial recognition (Hu et al., 2015) and medical diagnosis (Li et al., 2014). However, in many applications, captured images, such as real noisy images, are not sufficient, and deep CNNs tend to perform poorly in image applications. For this reason, GANs (Radford, Metz, & Chintala, 2015)

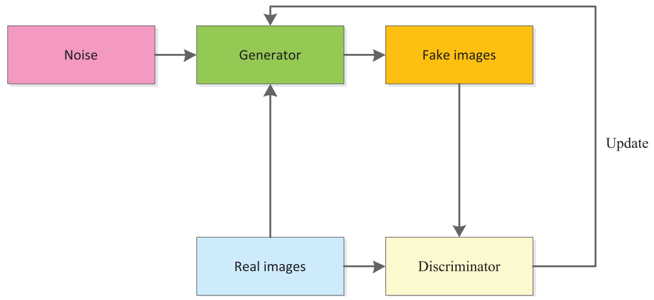

Fig. 6. Network architecture of GAN.

were developed. GANs consisted of two networks: generative and discriminative networks. The generative network (also referred to as the generator) is used to generate samples, according to input samples. The discriminative network (also called the discriminator) is used to judge the truth of both input samples and generated samples. The two networks are adversarial. Note that if the discriminator can accurately distinguish real samples and generate samples from generator, the trained model is regarded as finished. The network architecture of the GAN can be seen in Fig. 6. Due to its ability to construct supplemental training samples, the GAN is very effective for small sample tasks, such as facial recognition (Tran, Yin, & Liu, 2017) and complex noisy image denoising (Chen, Chen et al., 2018). These mentioned CNNs are basic networks for image denoising.

2.4. Hardware and software used in deep learning

One reason for the success of deep learning is the GPU. The GPU uses the CUDA (Nvidia, 2011), OpenCL (Stone, Gohara, & Shi, 2010) and cuDNN (Chetlur et al., 2014) platforms to strengthen its parallel computing ability, which exceeds the speed of the CPU by 10 to 30 times. The GPU consists of an NVIDIA consumer line of graphics cards (i.e., GTX 680, GTX 980, GTX 1070, GTX 1070Ti, GTX1080, GTX 1080Ti, RTX 2070, RTX 2080, RTX 2080Ti, Tesla K40c, Tesla K80, Quadro M6000, Quadro GP100, Quadro P6000 and Tesla V100) and AMD (i.e., Radeon Vega 64 and FE) (Kutzner, 2019).

Deep learning software can provide interfaces to call the GPU. Popular software packages include:

(1) Caffe (Jia et al., 2014) based on C++, provides C++, Python and Matlab interfaces, which can also run on both the CPU and GPU. It is widely used for object detection tasks. However, it requires developers to master C++.

(2) Theano (Bergstra et al., 2010) is a compiler of math expressions for dealing with large-scale neural networks. Theano provides a Python interface and is used in image super-resolution, denoising and classification.

(3) Matconvnet (Vedaldi & Lenc, 2015) offers the Matlab interface. It is utilized in image classification, denoising and super-resolution, and video tracking. However, it requires Matlab mastery.

(4) TensorFlow (Abadi et al., 2016) is a relatively high-order machine learning library. It is faster than Theano for compilation. TensorFlow offers C++ and Python interfaces and is used in object detection, image classification, denoising and super-resolution.

(5) Keras (Chollet et al., 2015) based on TensorFlow and Theano is implemented in Python and offers a Python interface. It can be used in image classification, object detection, image resolution, image denoising and action recognition.

(6) PyTorch (Paszke et al., 2017) is implemented in Python and offers a Python interface. It is employed in image classification, object detection, image segmentation, action recognition, image super-resolution, image denoising and video tracking.

3. Deep learning techniques in image denoising

3.1. Deep learning techniques for additive white noisy-image denoising

Due to the insufficiency of real noisy images, additive white noisy images (AWNIs) are widely used to train the denoising model (Jin, McCann, Froustey, & Unser, 2017). AWNIs include Gaussian, Poisson, Salt, Pepper and multiplicative noisy images (Farooque & Rohankar, 2013). There are several deep learning techniques for AWNI denoising, including CNN/NN; the combination of CNN/NN and common feature extraction methods; and the combination of the optimization method and CNN/NN.

3.1.1. CNN/NN for AWNI denoising

Automatic feature extraction methods can play a major role in reducing the computational costs for image applications (Lu et al., 2018; Ren et al., 2019; Yang, Zhang, Xu, & Yang, 2012). For this reason, CNNs have been developed for image denoising (Liu, Wen, Liu, Wang and Huang, 2017; McCann, Jin, & Unser, 2017). Zhang, Zuo, Chen et al. (2017) proposed a model as well as a DnCNN to deal with multiple low-level vision tasks, i.e., image denoising, super-resolution and deblocking through CNN, batch normalization (Ioffe & Szegedy, 2015) and residual learning techniques (He et al., 2016). Bae, Yoo, and Chul Ye (2017), Jifara, Jiang, Rho, Cheng, and Liu (2019) and Wang, Sun and Hu (2017) also presented a residual learning into deeper CNN for image denoising. However, the deeper CNN technique relied on a deeper layer rather than a shallow layer, which resulted in a long-term dependency problem. Several signal-base methods were proposed to resolve this problem. Tai, Yang, Liu, and Xu (2017) exploited recursive and gate units to adaptively mine more accurate features and recover clean images. Inspired by a low-rank Hankel matrix in low-level vision, Ye, Han, and Cha (2018) provided convolution frames to explain the connection between signal processing and deep learning by convolving local and nonlocal bases. For solving insufficient noisy images (i.e., hyperspectral and medical images), several recent works have attempted to extract more useful information through the use of improved CNNs (Chang, Yan, Fang, Zhong, & Liao, 2018; Heinrich, Stille, & Buzug, 2018; Liu & Lee, 2019; Yu, Liu, Wei, Fu, & Liu, 2018). For example, Yuan, Zhang, Li, Shen and Zhang (2018) combined a deep CNN, residual learning and multiscale knowledge to remove the noise from hyperspectral-noisy images. However, these proposed CNNs led to the likelihood of increased computational costs and memory consumption, which was not conducive for real-world applications. To address this phenomenon, Gholizadeh-Ansari, Alirezaie, and Babyn (2018) utilized dilated convolutions (Gashi, Pereira, & Vterkovska, 2017) to enlarge the receptive field and reduce the depth of network without incurring extra costs for CT image denoising. Su, Lian, Zhang, Shi, and Fan (2019) proposed a residual network via multi-scale cross-path concatenation to suppress the noise. Most of the above methods relied on improved CNNs to deal with the noise. Therefore, designing network architectures is important for image denoising (Li, Yang and Yong, 2018; Park, Kim, & Cho, 2018).

Changing network architectures involves the following methods (Mafi et al., 2018; Ren, Zuo, Hu, Zhu and Meng, 2019; Yu, Ma, & Wang, 2019): fusing features from multiple inputs of a CNN; changing the loss function; increasing depth or width of the CNN; adding some auxiliary plug-ins into CNNs; and introducing skip connections or cascade operations into CNNs. Specifically, the first method includes three types: different parts of one sample as multiple inputs from different networks (Abbasi, Monadjemi, Fang, Rabbani, & Zhang, 2019); different perspectives for the one sample as input, such as multiple scales (Chen, Xu, 2018; Jeon, Jeong, Son, & Yang, 2018); and different channels of a CNN as input (Jiang et al., 2018). The second method involves the design of different loss functions according to the characteristics of nature images to extract more robust features (Aljadaany, Pal, & Savvides, 2019). For example, Chen et al. (2018) jointed Euclidean and perceptual loss functions to mine more edge information for image denoising. The third method enlarged the receptive field size to improve denoising performance via increasing the depth or width of the network (Sheremet, Sheremet, Sadovoi, & Sokhina, 2018; Uchida, Tanaka, & Okutomi, 2018; Zarshenas & Suzuki, 2018). The fourth method applied plug-ins, such as activation function, dilated convolution, fully connected layer and pooling operations, to enhance the expressive ability of the CNN (Panda, Naskar, & Pal, 2018; Pardasani & Shreemali, 2018; Priyanka & Wang, 2019). The fifth method utilized skip connections (Anwar, Huynh, & Porikli, 2017; Chen, Xiong, Tian and Wu, 2018; Couturier, Perrot, & Salomon, 2018; Xiao, Guo, & Zhuang, 2018) or cascade operations (Chen, Yu, Jiang, Peng, & Chen, 2019; Su et al., 2019) to provide complementary information for the deep layer in a CNN. Table 1 provides an overview of CNNs for AWNI denoising.

3.1.2. CNN/NN and common feature extraction methods for AWNI denoising

Feature extraction is used to represent the entire image in image processing, and it is important for machine learning (Liang, Zhang, Lu, Guo, & Luo, 2019; Lu, Wong, Lai, & Li, 2019; Yang, Chu, Zhang, Xu, & Yang, 2013). However, because deep learning techniques are black box techniques, they do not allow the choice of features, and therefore cannot guarantee that the obtained features are the most robust (Shwartz-Ziv & Tishby, 2017; Wei, Xia, & Zhang, 2019). Motivated by problem, researches embedded common feature extraction methods into CNNs for the purpose of image denoising. They did this for five reasons: weak edge-information noisy images, non-linear noisy images, high dimensional noisy images and non-salient noisy images, and high computational costs.

For weak edge-information noisy images, CNN with transformation domain methods were proposed by Guan, Lai, and Xiong (2019), Li, Wu and Jin (2018), Liu, Zhang, Zhang, Lin and Zuo (2018), Latif, Iskandar, Alghazo, Butt, and Khan (2018) and Yang and Sun (2017). However, they were not effective in removing the noise. Specifically, in Liu, Zhang et al. (2018), the proposed solution used the wavelet method and U-net to eliminate the gridding effect of dilated convolutions on enlarging the receptive field for image restoration.

For non-linear noisy images, CNNs with kernel methods proved useful (Bako et al., 2017; Xu, Li, & Sun, 2019). These methods mostly consisted of three steps (Mildenhall et al., 2018). The first step used CNN to extract features. The second step utilized the kernel method to convert obtained non-linear features into linearity. The third step exploited the residual learning to construct the latent clean image.

For high dimensional noisy images, the combination of CNN and the dimensional reduction method was proposed (Guo, Sun, Jian, & Zhang, 2018; Xie, Li, & Jia, 2018). For example, Khaw, Soon, Chuah, and Chow (2017) used a CNN with principal component analysis (PCA) for image denoising. This consisted of three steps. The first step used convolution operations to extract features. The second step utilized the PCA to reduce the dimension of the obtained features. The third step employed convolutions to deal with the obtained features from the PCA and to reconstruct a clean image.

For non-salient noisy images, signal processing can guide the CNN in extracting salient features (Abbasi et al., 2019; Jia, Chai, Guo, Huang, & Zhao, 2018; Kadimesetty, Gutta, Ganapathy, & Yalavarthy, 2018; Ran et al., 2019). Specifically, skip connection is a typical operation of signal processing (Kadimesetty et al., 2018).

For tasks involving high computational costs, a CNN with relations nature of pixels from an image was very effective in decreasing complexity (Abbasi et al., 2019; Ahn & Cho, 2017; Ahn et al., 2018). For example, Ahn and Cho (2017) used a CNN with non-local self-similarity (NSS) to filter the noise, where similar characteristics of the given noisy image can accelerate the speed of extraction feature and reduce computational costs.

More detailed information on these methods mentioned can be found in Table 2.

3.1.3. Combination of optimization method and CNN/NN for AWNI denoising

Machine learning uses optimization techniques (Hsu & Lin, 2017; Li et al., 2020) and discriminative learning methods (Li et al., 2019; Liu & Fang, 2017) to deal with image applications. Although optimization methods have good performance on different low-level vision tasks, these methods need manual setting parameters, which are time-consuming (Tian, Xu, Zuo et al., 2020; Tian et al., 2020). The discriminative learning methods are fast in image restoration. However, they are not flexible for low-level vision tasks. To achieve a tradeoff between efficiency and flexibility, a discriminative learning optimization-based method (Bigdeli & Zwicker, 2017; Meinhardt, Moller, Hazirbas, & Cremers, 2017) was presented for image applications, such as image denoising. CNNs with prior knowledge via regular term of loss function is a common method in image denoising (Hongqiang, Shiping, Yuelei, & Mingming, 2018), which can be divided two categories: improvement of denoising speed and improvement of denoising performance.

For improving denoising speed, an optimization method using a CNN was an effective tool for rapidly finding the optimal solution in image denoising (Cho & Kang, 2018; Fu, Zhao, Li, Wang, & Ren, 2019). For example, a GAN with the maximum a posteriori (MAP) method was used to estimate the noise and deal with other tasks, such as image inpainting and super-resolution (Yeh et al., 2018). An experience-based greed algorithm and transfer learning strategies with a CNN can accelerate a genetic algorithm to obtain a clean image (Liu, Li, El Basha and Fang, 2018). Noisy image and noise level mapping were inputs of the CNN, which had faster execution in predicting the noise (Tassano, Delon, & Veit, 2019a).

For improving denoising performance, a CNN combined optimization method was used to make a noisy image smooth (Gondara & Wang, 2017; Heckel et al., 2018; Jiao et al., 2017). A CNN with total variation denoising reduced the effect of noise pixels (Wang, Qin et al., 2017). Combining the Split Bergman iteration algorithm and CNN (Li & Wu, 2019) can enhance pixels through image depth to obtain a latent clean image. A dual-stage CNN with feature matching can better recover the detailed information of the clean image, especially noisy images (Sun et al., 2018). The GAN with the nearest neighbor algorithm was effective in filtering out noisy images from clean images (ZhiPing et al., 2018). A combined CNN used wavefront coding to enhance the pixels of latent clean images via the transform domain (Du et al., 2018). Other effective denoising methods are shown in Gong et al. (2018), Khan et al. (2019) and Liu et al. (2019). Table 3 shows detailed information about the combination of the optimization methods and CNN/NN in AWNI denoising.

3.2. Deep learning techniques for real noisy image denoising

There are mainly two types of deep learning techniques for image denoising: single end-to-end CNN and the combination of prior knowledge and CNN.

For the first method, changing the network architecture is an effective way to remove the noise from the given real corrupted

Table 1
CNN/NN for AWNI denoising.

References	Methods	Applications	Key words (remarks)
Zhang, Zuo, Chen et al. (2017)	CNN	Gaussian image denoising, super-resolution and JPEG deblocking	CNN with residual learning, and BN for image denoising
Wang, Sun et al. (2017)	CNN	Gaussian image denoising	CNN with dilated convolutions, and BN for image denoising
Bae et al. (2017)	CNN	Gaussian image denoising, super-resolution	CNN with wavelet domain, and residual learning (RL) for image restoration
Jifara et al. (2019)	CNN	Medical (X-ray) image restoration	Improved Unet from iterative shrinkage idea for medical image restoration
Tai et al. (2017)	CNN	Gaussian image denoising, super-resolution and JPEG deblocking	CNN with recursive unit, gate unit for image restoration
Anwar et al. (2017)	CNN	Gaussian image denoising	CNN with fully connected layer, RL and dilated convolutions for image denoising
Jin et al. (2017)	CNN	Inverse problems (i.e., denoising, deconvolution, super-resolution)	CNN for inverse problems
Ye et al. (2018)	CNN	Inverse problems (i.e., Gaussian image denoising, super-resolution)	Signal processing ideas guide CNN for inverse problems
Yuan, Zhang et al. (2018)	CNN	Hyper-spectral image denoising	CNN with multiscale, multilevel features techniques for hyper-spectral image denoising
Jiang, Dou et al. (2018)	CNN	Gaussian image denoising	Multi-channel CNN for image denoising
Chang et al. (2018)	CNN	Hyper-spectral image (HSI) denoising, HIS restoration	CNN consolidated spectral and spatial coins for hyper-spectral image denoising
Jeon et al. (2018)	CNN	Speckle noise reduction from digital holographic images	Speckle noise reduction of digital holographic image from Multi-scale CNN
Gholizadeh-Ansari et al. (2018)	CNN	Low-dose CT image denoising, X-ray image denoising	CNN with dilated convolutions for low-dose CT image denoising
Uchida et al. (2018)	CNN	Non-blind image denoising	CNN with residual learning for non-blind image denoising
Xiao et al. (2018)	CNN	Stripe noise reduction of infrared cloud images	CNN with skip connection for infrared-cloud-image denoising
Chen et al. (2018)	CNN	Gaussian image denoising, blind denoising	CNN based on RL and perceptual loss for edge enhancement
Yu et al. (2019)	CNN	Seismic, random, linear and multiple noise reduction of images	A survey on deep learning for three applications
Yu et al. (2018)	CNN	Optical coherence tomography (OCT) image denoising	GAN with dense skip connection for optical coherence tomography image denoising
Li, Yang et al. (2018)	CNN	Ground-roll noise reduction	An overview of deep learning techniques on ground-roll noise
Abbasi et al. (2019)	CNN	OCT image denoising	Fully CNN with multiple inputs, and RL for OCT image denoising
Zarshenas and Suzuki (2018)	CNN	Gaussian noisy image denoising	Deep CNN with internal and external residual learning for image denoising
Chen, Xiong et al. (2018)	CNN	Gaussian noisy image denoising	CNN with recursive operations for image denoising
Panda et al. (2018)	CNN	Gaussian noisy image denoising	CNN with exponential linear units, and dilated convolutions for image denoising
Sheremet et al. (2018)	CNN	Image denoising from info-communication systems	CNN on image denoising from info-communication systems
Chen, Xu et al. (2018)	CNN	Aerial-image denoising	CNN with multi-scale technique, and RL for aerial-image denoising
Pardasani and Shreemali (2018)	CNN	Gaussian, Poisson or any additive-white noise reduction	CNN with BN for image denoising
Couturier et al. (2018)	NN	Gaussian and multiplicative speckle noise reduction	Encoder–decoder network with multiple skip connections for image denoising
Park et al. (2018)	CNN	Gaussian noisy image denoising	CNN with dilated convolutions for image denoising
Priyanka and Wang (2019)	CNN	Gaussian noisy image denoising	CNN with symmetric network architecture for image denoising
Su et al. (2019)	CNN	Poisson-noise-image denoising	CNN with multi scale, and multiple skip connections for Poisson image denoising
Tripathi, Lipton, and Nguyen (2018)	CNN	Gaussian noisy image denoising	GAN for image denoising
Zheng, Duan, Tang, Wang, and Zhou (2019)	CNN	Gaussian noisy image denoising	CNN for image denoising
Tian et al. (2019)	CNN	Gaussian noisy image denoising	CNN for image denoising
Remez, Litany, Giryes, and Bronstein (2018)	CNN	Gaussian and Poisson image denoising	CNN for image denoising
Tian, Xu and Zuo (2020)	CNN	Gaussian image denoising and real noisy image denoising	CNN with BRN, RL and dilated convolutions for image denoising
Tian et al. (2020)	CNN	Gaussian image denoising, blind denoising and real noisy image denoising	CNN with attention mechanism and sparse method for image denoising
Tian et al. (2020)	CNN	Gaussian image denoising, blind denoising and real noisy image denoising	Two CNNs with sparse method for image denoising

image. Multiscale knowledge is effective for image denoising. For example, a CNN consisting of convolution, ReLU and RL employed different phase features to enhance the expressive ability of the low-light image denoising model (Tao et al., 2017). To overcome the blurry and false image artifacts, a dual U-Net with skip connection was proposed for computed tomography (CT) image reconstruction (Han & Ye, 2018). To address the problem of resource-constraints problem, Tian, Xu, Zuo (2020) used

Table 2
CNN/NN and common feature extraction methods for AWNI denoising.

References	Methods	Applications	Key words (remarks)
Su et al. (2019)	CNN	Monte Carlo-rendered images denoising	CNN with kernel method for estimating noise pixels
Ahn and Cho (2017)	CNN	Gaussian image denoising	CNN with NSS for image denoising
Khaw et al. (2017)	CNN	Impulse noise reduction	CNN with PCA for image denoising
Vogel and Pock (2017)	CNN	Gaussian image denoising	U-net with multi scales technique for image denoising
Mildenhall et al. (2018)	NN	Low-light synthetic noisy image denoising, real noise	Encoder–decoder with multi scales, and kernel method for image denoising
Liu, Zhang et al. (2018)	CNN	Gaussian image denoising, super-resolution and JPEG deblocking	U-net with wavelet for image restoration
Yang and Sun (2017)	CNN	Gaussian image denoising	CNN with BM3D for image denoising
Guo et al. (2018)	CNN	Image blurring and denoising	CNN with RL, and sparse method for image denoising
Jia et al. (2018)	CNN	Gaussian image denoising	CNN with multi scales, and dense RL operations for image denoising
Ran et al. (2019)	CNN	OCT image denoising, OCT image super-resolution	CNN with multi views for image restoration
Lu, Lai et al. (2018)	CNN	Medical image denoising, stomach pathological image denoising	CNN consolidated wavelet for medical image denoising
Ahn, Kim, Park, and Cho (2018)	CNN	Gaussian image denoising	CNN with NSS for image denoising
Xie et al. (2018)	CNN	Hyper-spectral image denoising	CNN with RL, and PCA for low-dose CT image denoising
Kadimesetty et al. (2018)	CNN	Low-Dose computed tomography (CT) image denoising	CNN with RL, batch normalization (BN) for medical image denoising
Guan et al. (2019)	CNN	Stripe noise reduction	CNN with wavelet-image denoising
Abbasi et al. (2019)	NN	3D magnetic resonance image denoising, medical image denoising	GAN based on encoder–decoder and RL for medical denoising
Xu et al. (2019)	CNN	Synthetic and real noisy and video denoising	CNN based on deformable kernel for image and video denoising

Table 3
The combination of the optimization method and CNN/NN for AWNI denoising.

References	Methods	Applications	Key words (remarks)
Hongqiang et al. (2018)	CNN	Gaussian image denoising	Auto-Encoder with BN, and ReLU for image denoising
Cho and Kang (2018)	CNN	Gaussian image denoising	CNN with separable convolution, and gradient prior for image denoising
Fu et al. (2019)	CNN	Salt and pepper noise removal	CNN with non-local switching filter for salt and pepper noise
Yeh et al. (2018)	CNN	Image denoising super-resolution and inpainting	GAN with MAP for image restoration
Liu, Li et al. (2018)	CNN	Medical image denoising, computed tomography perfusion for image denoising	CNN with genetic algorithm for medical image denoising
Tassano et al. (2019a)	CNN	Gaussian image denoising	CNN with noise level, upscaling, downscaling operation for image denoising
Heckel, Huang, Hand, and Voroninski (2018)	CNN	Image denoising	CNN with deep prior for image denoising
Jiao, Tu, He, and Lau (2017)	CNN	Gaussian image denoising, image inpainting	CNN with inference, residual operation for image restoration
Wang, Qin and Zhu (2017)	CNN	Image denoising	CNN with total variation for image denoising
Li and Wu (2019)	CNN	Image painting	CNN with split Bergman iteration algorithm for image painting
Sun, Kottayil, Mukherjee, and Cheng (2018)	CNN	Gaussian image denoising	GAN with skip-connections, and ResNet blocks for image denoising
ZhiPing, YuanQi, Yi, and XiangBo (2018)	CNN	Gaussian image denoising	GAN with multiscale for image denoising
Du et al. (2018)	CNN	Gaussian image denoising	CNN with wavelet for medical image restoration
Liu, Suganuma, Sun, and Okatani (2019)	CNN	Gaussian image denoising, real noisy image denoising, rain removal	Dual CNN with residual operations for image restoration
Khan, Khan, and Shin (2019)	CNN	Symbol denoising	CNN with quadrature amplitude modulation for symbol denoising
Zhang, Zhang, Liu and Wang (2019)	CNN	Image Poisson denoising	CNN with variance-stabilizing transformation for Poisson denoising
Cruz, Foi, Katkovnik, and Egiazarian (2018)	CNN	Gaussian image denoising	CNN with nonlocal filter for image denoising
Jia, Liu, Feng, and Zhang (2019)	CNN	Gaussian image denoising	CNN based on a fractional-order differential equation for image denoising

a dual CNN with batch renormalization (Ioffe, 2017), RL and dilated convolutions to deal with real noisy images. Based on nature of light images, two CNNs utilized anisotropic parallax analysis to generate structural parallax information for real noisy images (Chen, Hou and Chau, 2018). Using a CNN to resolve remote sensing (Jian, Zhao, Bai, & Fan, 2018) and medical images (Khoroushadi & Sadegh, 2018) under low-light conditions proved effective (Jiang, Jing, Hu, Ge and Xiao, 2018). To extract more detailed information, recurrent connections were used to enhance the representative ability to deal with corrupted images in the real world (Godard, Matzen, & Uyttendaele, 2018; Zhao, Ma, Li and Yu, 2019). To deal with unknown real noisy images, a residual structure was utilized to facilitate low-frequency features, and then, an attention mechanism (Tian, Xu, Li et al., 2020) could be applied to extract more potential features from channels (Anwar & Barnes, 2019). To produce the noisy image, a technique used imitating cameral pipelines to construct the degradation model in order to filter the real noisy images (Jaroensri, Biscarrat, Aittala, &

Table 4
CNNs for real noisy image denoising.

References	Methods	Applications	Key words (remarks)
Tao, Zhu, Xiang et al. (2017)	CNN	Real noisy image denoising, low-light image enhancement	CNN with ReLU, and RL for real noisy image denoising
Chen, Chen et al. (2018)	CNN	Real noisy image denoising, blind denoising	GAN for real noisy image denoising
Han and Ye (2018)	CNN	CT image reconstruction	U-Net with skip connection for CT image reconstruction
Chen, Hou et al. (2018)	CNN	Real noisy image denoising	CNNs with anisotropic parallax analysis for real noisy image denoising
Jian et al. (2018)	CNN	Low-light remote sense image denoising	CNN for image denoising
Khoroushadi and Sadegh (2018)	CNN	Medical image denoising, CT image denoising	CNN for image denoising
Jiang, Jing et al. (2018)	CNN	Low-light image enhancement	CNN with symmetric pathways for low-light image enhancement
Godard et al. (2018)	CNN	Real noisy image denoising	CNN with recurrent connections for real noisy image denoising
Zhao, Ma et al. (2019)	CNN	Real noisy image denoising	CNN with recurrent connections for real noisy image denoising
Anwar and Barnes (2019)	CNN	Real noisy image denoising	CNN with RL, attention mechanism for real noisy image denoising
Wang et al. (2019)	CNN	Real noisy image denoising	CNN for real noisy image denoising
Green, Marom, Konen, Kiryati, and Mayer (2018)	CNN	CT image denoising, real noisy image denoising	CNN for real noisy image denoising
Brooks et al. (2019)	CNN	Real noisy image denoising	CNN with image processing pipeline for real noisy image denoising
Tian, Xu, Zuo (2020)	CNN	Gaussian image denoising and real noisy image denoising	CNN with BRN, RL and dilated convolutions for image denoising
Tian, Xu, Li et al. (2020)	CNN	Gaussian image denoising, blind denoising and real noisy image denoising	CNN with attention mechanism and sparse method for image denoising
Tian, Xu, Zuo, Du et al. (2020)	CNN	Gaussian image denoising, blind denoising and real noisy image denoising	Two CNNs with sparse method for image denoising
Cui et al. (2019)	CNN	Positron emission tomography image denoising, real noisy image denoising	Unsupervised CNN for unpair real noisy image denoising
Yan et al. (2019)	CNN	Real noisy image denoising	Self-supervised GAN for unpair real noisy image denoising
Broaddus, Krull, Weigert, Schmidt, and Myers (2020)	CNN	Blind denoising and real noisy image denoising	Self-supervised CNN for unpair fluorescence microscopy image denoising
Li, Hsu et al. (2020)	CNN	CT noisy image denoising	Self-supervised CNN with attention mechanism for unpair CT image denoising
Hendriksen et al. (2020)	CNN	CT noisy image denoising	Self-supervised CNN for unpair CT image denoising
Wu, Ren, and Li (2020)	CNN	CT noisy image denoising	Self-supervised CNN for unpair dynamic CT image denoising

Durand, 2019). To tackle the problem of unpairing noisy images, an unsupervised learning method embedded into the CNN proved effective in image denoising (Cui et al., 2019). The self-consistent GAN (Yan, Tan, Yang, & Feng, 2019) first used a CNN to estimate the noise of the given noisy image as a label, and then, applied another CNN and the obtained label to remove the noise for other noisy images. This concept has also been extended to general CNNs. The Noise2Inverse method used a CNN to predict the value of a noisy pixel, according to its surrounding noisy pixels (Hendriksen, Pelt, & Batenburg, 2020). The attention mechanism merged into a 3D self-supervised network can improve the efficiency of removing the noise from medical noisy images (Li, Hsu, Xie, Cong and Gao, 2020). More detailed information about the above research is shown in Table 4.

The method combining CNN and prior knowledge can better deal with both speed and complex noise task in real noisy images. Zhang, Zuo, Gu and Zhang (2017) proposed using half quadratic splitting (HQS) and CNN to estimate the noise from the given real noisy image. Guo et al. (2019) proposed a three-phase denoising method. The first phase used a Gaussian noise and in-camera processing pipeline to synthesize noisy images. The synthetic and real noisy images were merged to better represent real noisy images. The second phase used a sub-network with asymmetric and total variation losses to estimate the noise of real noisy image. The third phase exploited the original noisy image and estimated noise to recover the latent clean image. To address the problem of unpaired noisy images, the combination of CNN and prior knowledge in a semi-supervised way was developed (Meng et al., 2020). A hierarchical deep GAN (HD-GAN) first used a cluster algorithm to classify multiple categories of each patient's CT, then built a dataset by collecting the images in the same categories from different patients. Finally, the GAN was used to deal with the obtained dataset for image denoising and classification (Choi et al., 2019). A similar method performed well in 3D mapping (Shantia, Timmers, Schomaker, & Wiering, 2015).

A CNN with channel prior knowledge was effective for low-light image enhancement (Tao et al., 2017). Table 5 shows the detailed information about the above research.

3.3. Deep learning techniques for blind denoising

In the real world, images are easily corrupted and noise is complex. Therefore, blind denoising techniques are important (Loo Tiang Kuan, 2017). An FFDNet (Zhang et al., 2018a) used noise level and noise as the input of CNN to train a denoiser for unknown noisy images. Subsequently, several methods were proposed to solve the problem of blind denoising. An image device mechanism proposed by Isogawa, Ida, Shiodera, and Takeguchi (2017) utilized soft shrinkage to adjust the noise level for blind denoising. For unpaired noisy images, using CNNs to estimate noise proved effective (Soltanayev & Chun, 2018). Yang, Liu, Song, and Li (2017) used known noise levels to train a denoiser, then utilized this denoiser to estimate the level of noise. To resolve the problem of random noise attenuation, a CNN with RL was used to filter complex noise (Si & Yuan, 2018; Zhang, Liu, Wang, Chen and Wang, 2018). Changing the network architecture can improve

Table 5
CNNs for real noisy image denoising.

References	Methods	Applications	Key words (remarks)
Zhang, Zuo, Gu et al. (2017)	CNN	Real-noisy image denoising	CNN with HQS for real noisy image
Guo et al. (2019)	CNN	Real-noisy image denoising	CNN and cameral processing pipeline for real noisy image
Tao, Zhu, Song et al. (2017)	CNN	Low-light image enhancement	CNN with channel prior for low-light image enhancement
Ma et al. (2018)	CNN	Tomography image denoising	GAN with edge-prior for CT image denoising
Yue, Yong, Zhao, Meng, and Zhang (2019)	CNN	Real-noisy image denoising, blind denoising	CNN with variational inference for blind denoising and real-noisy image denoising
Song, Zhu, and Du (2019)	CNN	Real noisy image denoising	CNN with dynamic residual dense block for real noisy image denoising
Lin, Li, Liu, and Li (2019)	CNN	Real noisy image denoising	GAN with attentive mechanism and noise domain for real noisy image denoising
Meng et al. (2020)	CNN	Real noisy image denoising	CNN with semi-supervised learning for medical noisy image denoising
Shantia et al. (2015)	CNN	Real noisy image denoising	CNN with semi-supervised learning for 3D map
Choi et al. (2019)	CNN	Real noisy image denoising	CNN with semi-supervised learning for medical noisy image denoising

Table 6
Deep learning techniques for blind denoising.

References	Methods	Applications	Key words (remarks)
Zhang et al. (2018a)	CNN	Blind denoising	CNN with varying noise level for blind denoising
Isogawa et al. (2017)	CNN	Blind denoising	CNN with soft shrinkage for blind denoising
Soltanayev and Chun (2018)	CNN	Blind denoising	CNN for unpaired noisy images
Yang et al. (2017)	CNN	Blind denoising	CNNs with RL for blind denoising
Zhang, Liu et al. (2018)	CNN	Blind denoising, random noise	CNN with RL for blind denoising
Si and Yuan (2018)	CNN	Blind denoising, random noise	CNN for image denoising
Jiang, Jing et al. (2018)	NN	Blind denoising	Auto-encoder for blind denoising
Godard et al. (2018)	CNN	Blind denoising, complex noisy image denoising	Cascaded CNNs for blind denoising
Yang et al. (2017)	CNN	Blind denoising	GAN for blind image denoising
Tian, Xu, Li et al. (2020)	CNN	Gaussian image denoising, blind denoising and real noisy image denoising	CNN with attention mechanism and sparse method for image denoising

the denoising performance for blind denoising. Majumdar (2018) proposed the use of an auto-encoder to tackle unknown noise. For mixed noise, cascaded CNNs were effective in removing the additive white Gaussian noise (AWGN) and impulse noise (Abiko & Ikehara, 2019). Table 6 displays more information about these denoising methods.

3.4. Deep learning techniques for hybrid noisy image denoising

In the real world, captured images are affected by complex environments. Motivated by that, several researchers proposed hybrid-noisy-image denoising techniques. Li et al. (2018) proposed the combination of CNN and warped guidance to resolve the questions of noise, blur and JPEG compression. Zhang, Zuo, and Zhang (2018b) used a model to deal with multiple degradations, such as noise, blur kernel and low-resolution image. To enhance the raw sensor data, Kokkinos and Lefkimmiatis (2019) presented a residual CNN with an iterative algorithm for image demosaicing and denoising. To handle arbitrary blur kernels, Zhang, Zuo et al. (2019) proposed to use cascaded deblurring and single-image super-resolution (SISR) networks to recover plug-and-play super-resolution images. These hybrid noisy image denoising methods are presented in Table 7.

Table 7
Deep learning techniques for hybrid noisy image denoising.

References	Methods	Applications	Key words (remarks)
Li, Liu et al. (2018)	CNN	Noise, blur kernel, JPEG compression	The combination of CNN and warped guidance for multiple degradations
Zhang et al. (2018b)	CNN	Noise, blur kernel, low-resolution image	CNN for multiple degradations
Kokkinos and Lefkimmiatis (2019)	CNN	Image demosaicing and denoising	Residual CNN with iterative algorithm for image demosaicing and denoising

It is noted that an image carries finite information, which is not beneficial in real-world applications. To address this problem, burst techniques were developed (Xia, Perazzi, Gharbi, Sunkavalli, & Chakrabarti, 2019). However, the burst image suffered from the effects of noise and camera shake, which increased the difficulty of implementing the actual task. Recently, there has been much interest in deep learning technologies for burst image denoising, where the noise is removed frame by frame (Aittala & Durand, 2018). Recurrent fully convolutional deep neural networks can filter the noise for all frames in a sequence of arbitrary length (Godard et al., 2018). The combination of CNN and the kernel method can boost the denoising performance for burst noisy images (Marinč, Srinivasan, Gül, Hellge, & Samek, 2019; Mildenhall et al., 2018). In terms of complex background noisy images, an attention mechanism combined the kernel and CNN to enhance the effect of key features for burst image denoising, which can accelerate the training speed (Zhang, Jin, Xia, Huang, & Xiong, 2020). For low-light conditions, using a CNN to map a given burst noisy image to sRGB outputs can obtain a multi-frame denoising image sequence (Zhao, Ma et al., 2019). To reduce network complexity, a CNN with residual learning directly trained a denoising model rather than an explicit aligning procedure (Tan, Xiao, Lai, Liu, & Zhang, 2019). These burst denoising methods are listed in Table 8.

Table 8
Deep learning techniques for burst denoising.

References	Methods	Applications	Key words (remarks)
Xia et al. (2019)	CNN	Burst denoising	CNN for burst denoising
Aittala and Durand (2018)	CNN	Burst denoising	CNN for burst denoising
Godard et al. (2018)	CNN	Burst denoising	CNN for burst denoising
Marinč et al. (2019)	CNN	Burst denoising	CNN with kernel idea for burst denoising
Mildenhall et al. (2018)	CNN	Burst denoising	CNN with kernel idea for burst denoising
Zhang et al. (2020)	CNN	Burst denoising	CNN with kernel idea and attention idea for burst denoising
Zhao, Ma et al. (2019)	CNN	Burst denoising	CNN for burst denoising
Tan et al. (2019)	CNN	Burst denoising	CNN without explicit aligning procedure for burst denoising

Table 9
Deep learning techniques for video denoising.

References	Methods	Applications	Key words (remarks)
Sadda and Qarni (2018)	CNN	Medical noisy video	CNN for video denoising
Wang, Zhou, and Cheng (2020)	CNN	Additive white Gaussian and salt-and-pepper noisy video	CNN for video denoising
Chen, Song, and Yang (2016)	CNN	Additive white Poisson-Gaussian noisy video	CNN for video denoising
Davy, Ehret, Morel, Arias, and Facciolo (2018)	CNN	Additive white Gaussian noisy video	CNN with non-local idea for video denoising
Tassano, Delon, and Veit (2019b)	CNN	Additive white Gaussian noisy video	CNN with temporal information for video denoising
Ehret, Davy, Morel, Facciolo, and Arias (2019)	CNN	Blind video denoising	CNN with pre-trained technology for blind video denoising

Similar to burst images, video detection is decomposed into each frame. Therefore, deep learning techniques for additive white noisy-image denoising, real noisy image denoising, blind denoising, hybrid noisy image denoising are also suitable to video denoising (Sadda & Qarni, 2018; Wang et al., 2020). A recurrent neural network (Chen et al., 2016) utilized an end-to-end CNN to remove the noise from corrupted video. To improve video denoising, reducing the video redundancy is an effective method. A non-local patch idea fused CNN can efficiently suppress the noise for video and image denoising (Davy et al., 2018). A CNN combined temporal information to make a tradeoff between performance and training efficiency in video denoising (Tassano et al., 2019b). For blind video denoising, a two-stage CNN proved to be a good choice (Ehret et al., 2019). The first phase trained a video denoising model by fine-tuning a pre-trained AWGN denoising network (Ehret et al., 2019). The second phase obtained latent clean video by the obtained video denoising model. These video denoising methods are described in Table 9.

Table 10
PSNR (dB) of different methods on the BSD68 for different noise levels (i.e., 15, 25 and 50).

Methods	15	25	50
BM3D (Dabov et al., 2007)	31.07	28.57	25.62
WNNM (Gu et al., 2014)	31.37	28.83	25.87
EPLL (Zoran & Weiss, 2011)	31.21	28.68	25.67
MLP (Burger et al., 2012)	–	28.96	26.03
CSF (Schmidt & Roth, 2014)	31.24	28.74	–
TNRD (Chen & Pock, 2016)	31.42	28.92	25.97
ECNDNet (Tian et al., 2019)	31.71	29.22	26.23
RED (Mao et al., 2016)	–	–	26.35
DnCNN (Zhang, Zuo, Chen et al., 2017)	31.72	29.23	26.23
DDRN (Wang, Sun et al., 2017)	31.68	29.18	26.21
PHGMS (Bae et al., 2017)	31.86	–	26.36
MemNet (Tai et al., 2017)	–	–	26.35
EEDN (Chen et al., 2018)	31.58	28.97	26.03
NBCNN (Uchida et al., 2018)	31.57	29.11	26.16
NNC (Zarshenas & Suzuki, 2018)	31.49	28.88	25.25
ELDRN (Panda et al., 2018)	32.11	29.68	26.76
PSN-K (Aljadaany et al., 2019)	31.70	29.27	26.32
PSN-U (Aljadaany et al., 2019)	31.60	29.17	26.30
DDFN (Couturier et al., 2018)	31.66	29.16	26.19
CIMM (Anwar et al., 2017)	31.81	29.34	26.40
DWDN (Li, Wu et al., 2018)	31.78	29.36	–
MWCNN (Liu, Zhang et al., 2018)	31.86	29.41	26.53
BM3D-Net (Yang & Sun, 2017)	31.42	28.83	25.73
MPFE-CNN (Kadimesetty et al., 2018)	31.79	29.31	26.34
IRCNN (Zhang, Zuo, Gu et al., 2017)	31.63	29.15	26.19
FFDNet (Zhang et al., 2018a)	31.62	29.19	26.30
BRDNet (Tian, Xu, Zuo, 2020)	31.79	29.29	26.36
ETN (Wang, Qin et al., 2017)	31.82	29.34	26.32
ADNet (Tian, Xu, Li et al., 2020)	31.74	29.25	26.29
NN3D (Cruz et al., 2018)	–	–	26.42
FOCNet (Jia et al., 2019)	31.83	29.38	26.50
DudeNet (Tian, Xu, Zuo, Du et al., 2020)	31.78	29.29	26.31

Table 11
FSIM of different methods on the BSD68 for different noise levels (i.e., 15, 25 and 50).

Methods	15	25	50
BM3D (Dabov et al., 2007)	0.9894	0.9811	0.9629
MLP (Burger et al., 2012)	0.9671	0.9821	0.9344
TNRD (Chen & Pock, 2016)	0.9697	0.9820	0.9291
ECNDNet (Tian et al., 2019)	0.9911	0.9837	0.9686
IRCNN (Zhang, Zuo, Gu et al., 2017)	0.9905	0.9835	0.9700
BRDNet (Tian, Xu, Zuo, 2020)	0.9913	0.9841	0.9687
ADNet (Tian, Xu, Li et al., 2020)	0.9912	0.9837	0.9673

Table 12
PSNR (dB) of different methods on the Set12 for different noise levels (i.e., 15, 25 and 50).

Images	C.man	House	Peppers	Starfish	Monarch	Airplane	Parrot	Lena	Barbara	Boat	Man	Couple	Average
Noise level	$\sigma = 15$												
BM3D (Dabov et al., 2007)	31.91	34.93	32.69	31.14	31.85	31.07	31.37	34.26	33.10	32.13	31.92	32.10	32.37
WNNM (Gu et al., 2014)	32.17	35.13	32.99	31.82	32.71	31.39	31.62	34.27	33.60	32.27	32.11	32.17	32.70
EPLL (Zoran & Weiss, 2011)	31.85	34.17	32.64	31.13	32.10	31.19	31.42	33.92	31.38	31.93	32.00	31.93	32.14
CSF (Schmidt & Roth, 2014)	31.95	34.39	32.85	31.55	32.33	31.33	31.37	34.06	31.92	32.01	32.08	31.98	32.32
TNRD (Chen & Pock, 2016)	32.19	34.53	33.04	31.75	32.56	31.46	31.63	34.24	32.13	32.14	32.23	32.11	32.50
ECNDNet (Tian et al., 2019)	32.56	34.97	33.25	32.17	33.11	31.70	31.82	34.52	32.41	32.37	32.39	32.39	32.81
DnCNN (Zhang, Zuo, Chen et al., 2017)	32.61	34.97	33.30	32.20	33.09	31.70	31.83	34.62	32.64	32.42	32.46	32.47	32.86
PSN-K (Aljadaany et al., 2019)	32.58	35.04	33.23	32.17	33.11	31.75	31.89	34.62	32.64	32.52	32.39	32.43	32.86
PSN-U (Aljadaany et al., 2019)	32.04	35.03	33.21	31.94	32.93	31.61	31.62	34.56	32.49	32.41	32.37	32.43	32.72
CIMM (Anwar et al., 2017)	32.61	35.21	33.21	32.35	33.33	31.77	32.01	34.69	32.74	32.44	32.50	32.52	32.95
IRCNN (Zhang, Zuo, Gu et al., 2017)	32.55	34.89	33.31	32.02	32.82	31.70	31.84	34.53	32.43	32.34	32.40	32.40	32.77
FFDNet (Zhang et al., 2018a)	32.43	35.07	33.25	31.99	32.66	31.57	31.81	34.62	32.54	32.38	32.41	32.46	32.77
BRDNet (Tian, Xu, Zuo, 2020)	32.80	35.27	33.47	32.24	33.35	31.85	32.00	34.75	32.93	32.55	32.50	32.62	33.03
ADNet (Tian, Xu, Li et al., 2020)	32.81	35.22	33.49	32.17	33.17	31.86	31.96	34.71	32.80	32.57	32.47	32.58	32.98
DudeNet (Tian, Xu, Zuo, Du et al., 2020)	32.71	35.13	33.38	32.29	33.28	31.78	31.93	34.66	32.73	32.46	32.46	32.49	32.94
Noise level	$\sigma = 25$												
BM3D (Dabov et al., 2007)	29.45	32.85	30.16	28.56	29.25	28.42	28.93	32.07	30.71	29.90	29.61	29.71	29.97
WNNM (Gu et al., 2014)	29.64	33.22	30.42	29.03	29.84	28.69	29.15	32.24	31.24	30.03	29.76	29.82	30.26
EPLL (Zoran & Weiss, 2011)	29.26	32.17	30.17	28.51	29.39	28.61	28.95	31.73	28.61	29.74	29.66	29.53	29.69
MLP (Burger et al., 2012)	29.61	32.56	30.30	28.82	29.61	28.82	29.25	32.25	29.54	29.97	29.88	29.73	30.03
CSF (Schmidt & Roth, 2014)	29.48	32.39	30.32	28.80	29.62	28.72	28.90	31.79	29.03	29.76	29.71	29.53	29.84
TNRD (Chen & Pock, 2016)	29.72	32.53	30.57	29.02	29.85	28.88	29.18	32.00	29.41	29.91	29.87	29.71	30.06
ECNDNet (Tian et al., 2019)	30.11	33.08	30.85	29.43	30.30	29.07	29.38	32.38	29.84	30.14	30.03	30.03	30.39
DnCNN (Zhang, Zuo, Chen et al., 2017)	30.18	33.06	30.87	29.41	30.28	29.13	29.43	32.44	30.00	30.21	30.10	30.12	30.43
PSN-K (Aljadaany et al., 2019)	30.28	33.26	31.01	29.57	30.30	29.28	29.38	32.57	30.17	30.31	30.10	30.18	30.53
PSN-U (Aljadaany et al., 2019)	29.79	33.23	30.90	29.30	30.17	29.06	29.25	32.45	29.94	30.25	30.05	30.12	30.38
CIMM (Anwar et al., 2017)	30.26	33.44	30.87	29.77	30.62	29.23	29.61	32.66	30.29	30.30	30.18	30.24	30.62
IRCNN (Zhang, Zuo, Gu et al., 2017)	30.08	33.06	30.88	29.27	30.09	29.12	29.47	32.43	29.92	30.17	30.04	30.08	30.38
FFDNet (Zhang et al., 2018a)	30.10	33.28	30.93	29.32	30.08	29.04	29.44	32.57	30.01	30.25	30.11	30.20	30.44
BRDNet (Tian, Xu, Zuo, 2020)	31.39	33.41	31.04	29.46	30.50	29.20	29.55	32.65	30.34	30.33	30.14	30.28	30.61
ADNet (Tian, Xu, Li et al., 2020)	30.34	33.41	31.14	29.41	30.39	29.17	29.49	32.61	30.25	30.37	30.08	30.24	30.58
DudeNet (Tian, Xu, Zuo, Du et al., 2020)	30.23	33.24	30.98	29.53	30.44	29.14	29.48	32.52	30.15	30.24	30.08	30.15	30.52
Noise level	$\sigma = 50$												
BM3D (Dabov et al., 2007)	26.13	29.69	26.68	25.04	25.82	25.10	25.90	29.05	27.22	26.78	26.81	26.46	26.72
WNNM (Gu et al., 2014)	26.45	30.33	26.95	25.44	26.32	25.42	26.14	29.25	27.79	26.97	26.94	26.64	27.05
EPLL (Zoran & Weiss, 2011)	26.10	29.12	26.80	25.12	25.94	25.31	25.95	28.68	24.83	26.74	26.79	26.30	26.47
MLP (Burger et al., 2012)	26.37	29.64	26.68	25.43	26.26	25.56	26.12	29.32	25.24	27.03	27.06	26.67	26.78
TNRD (Chen & Pock, 2016)	26.62	29.48	27.10	25.42	26.31	25.59	26.16	28.93	25.70	26.94	26.98	26.50	26.81
ECNDNet (Tian et al., 2019)	27.07	30.12	27.30	25.72	26.82	25.79	26.32	29.29	26.26	27.16	27.11	26.84	27.15
DnCNN (Zhang, Zuo, Chen et al., 2017)	27.03	30.00	27.32	25.70	26.78	25.87	26.48	29.39	26.22	27.20	27.24	26.90	27.18
PSN-K (Aljadaany et al., 2019)	27.10	30.34	27.40	25.84	26.92	25.90	26.56	29.54	26.45	27.20	27.21	27.09	27.30
PSN-U (Aljadaany et al., 2019)	27.21	30.21	27.53	25.63	26.93	25.89	26.62	29.54	26.56	27.27	27.23	27.04	27.31
CIMM (Anwar et al., 2017)	27.25	30.70	27.54	26.05	27.21	26.06	26.53	29.65	26.62	27.36	27.26	27.24	27.46
IRCNN (Zhang, Zuo, Gu et al., 2017)	26.88	29.96	27.33	25.57	26.61	25.89	26.55	29.40	26.24	27.17	27.17	26.88	27.14
FFDNet (Zhang et al., 2018a)	27.05	30.37	27.54	25.75	26.81	25.89	26.57	29.66	26.45	27.33	27.29	27.08	27.32
BRDNet (Tian, Xu, Zuo, 2020)	27.44	30.53	27.67	25.77	26.97	25.93	26.66	29.73	26.85	27.38	27.27	27.17	27.45
ADNet (Tian, Xu, Li et al., 2020)	27.31	30.59	27.69	25.70	26.90	25.88	26.56	29.59	26.64	27.35	27.17	27.07	27.37
DudeNet (Tian, Xu, Zuo, Du et al., 2020)	27.22	30.27	27.51	25.88	26.93	25.88	26.50	29.45	26.49	27.26	27.19	26.97	27.30

4. Experimental results

4.1. Datasets

4.1.1. Training datasets

The training datasets are divided into two categories: gray-noisy and color-noisy images. Gray-noisy image datasets can be used to train Gaussian denoisers and blind denoisers. They included the BSD400 dataset (Bigdeli, Zwicker, Favaro, & Jin, 2017) and Waterloo Exploration Database (Ma et al., 2016). The BSD400 dataset was composed of 400 images in .png format, and was cropped into a size of 180 × 180 for training a denoising model. The Waterloo Exploration Database consisted of 4744 nature images with a .png format. Color-noisy images included the BSD432 (Zhang, Zuo, Chen et al., 2017), Waterloo Exploration Database and polyU-Real-World-Noisy-Images datasets (Xu, Li, Liang, Zhang and Zhang, 2018). Specifically, the polyU-Real-World-Noisy-Images consisted of 100 real noisy images with

Table 13
PSNR (dB) of different methods on the CBSD68, Kodak24 and McMaster for different noise levels (i.e., 15, 25, 35, 50 and 75).

Datasets	Methods	$\sigma = 15$	$\sigma = 25$	$\sigma = 35$	$\sigma = 50$	$\sigma = 75$
CBSD68	CBM3D (Dabov et al., 2007)	33.52	30.71	28.89	27.38	25.74
	DnCNN (Zhang, Zuo, Chen et al., 2017)	33.98	31.31	29.65	28.01	–
	DDRN (Wang, Sun et al., 2017)	33.93	31.24	–	27.86	–
	EEDN (Chen et al., 2018)	33.65	31.03	–	27.85	–
	DDFN (Couturier et al., 2018)	34.17	31.52	29.88	28.26	–
	CIMM (Anwar et al., 2017)	31.81	29.34	–	26.40	–
	BM3D-Net (Yang & Sun, 2017)	33.79	30.79	–	27.48	–
	IRCNN (Zhang, Zuo, Gu et al., 2017)	33.86	31.16	29.50	27.86	–
	FFDNet (Zhang et al., 2018a)	33.80	31.18	29.57	27.96	26.24
	BRDNet (Tian, Xu, Zuo, 2020)	34.10	31.43	29.77	28.16	26.43
	GPADCNN (Cho & Kang, 2018)	33.83	31.12	29.46	–	–
	FFDNet (Tassano et al., 2019a)	33.76	31.18	29.58	–	26.57
	ETN (Wang, Qin et al., 2017)	34.10	31.41	–	28.01	–
	ADNet (Tian, Xu, Li et al., 2020)	33.99	31.31	29.66	28.04	26.33
	DudeNet (Tian, Xu, Zuo, Du et al., 2020)	34.01	31.34	29.71	28.09	26.40
Kodak24	CBM3D (Dabov et al., 2007)	34.28	31.68	29.90	28.46	26.82
	DnCNN (Zhang, Zuo, Chen et al., 2017)	34.73	32.23	30.64	29.02	–
	IRCNN (Zhang, Zuo, Gu et al., 2017)	34.56	32.03	30.43	28.81	–
	FFDNet (Zhang et al., 2018a)	34.55	32.11	30.56	28.99	27.25
	BRDNet (Tian, Xu, Zuo, 2020)	34.88	32.41	30.80	29.22	27.49
	FFDNet (Tassano et al., 2019a)	34.53	32.12	30.59	–	27.61
	ADNet (Tian, Xu, Li et al., 2020)	34.76	32.26	30.68	29.10	27.40
	DudeNet (Tian, Xu, Zuo, Du et al., 2020)	34.81	32.26	30.69	29.10	27.39
McMaster	CBM3D (Dabov et al., 2007)	34.06	31.66	29.92	28.51	26.79
	DnCNN (Zhang, Zuo, Chen et al., 2017)	34.80	32.47	30.91	29.21	–
	IRCNN (Zhang, Zuo, Gu et al., 2017)	34.58	32.18	30.59	28.91	–
	FFDNet (Zhang et al., 2018a)	34.47	32.25	30.76	29.14	27.29
	BRDNet (Tian, Xu, Zuo, 2020)	35.08	32.75	31.15	29.52	27.72
	ADNet (Tian, Xu, Li et al., 2020)	34.93	32.56	31.00	29.36	27.53

Table 14
Running time of 13 popular denoising methods for the noisy images of sizes 256×256,512×512 and 1024×1024.

Methods	Device	256×256	512×512	1024×1024
BM3D (Dabov et al., 2007)	CPU	0.65	2.85	11.89
WNNM (Gu et al., 2014)	CPU	203.1	773.2	2536.4
EPLL (Zoran & Weiss, 2011)	CPU	25.4	45.5	422.1
MLP (Burger et al., 2012)	CPU	1.42	5.51	19.4
CSF (Schmidt & Roth, 2014)	CPU	2.11	5.67	40.8
CSF (Schmidt & Roth, 2014)	GPU	–	0.92	1.72
TNRD (Chen & Pock, 2016)	CPU	0.45	1.33	4.61
TNRD (Chen & Pock, 2016)	GPU	0.010	0.032	0.116
ECNDNet (Tian et al., 2019)	GPU	0.012	0.079	0.205
DnCNN (Zhang, Zuo, Chen et al., 2017)	CPU	0.74	3.41	12.1
DnCNN (Zhang, Zuo, Chen et al., 2017)	GPU	0.014	0.051	0.200
FFDNet (Zhang et al., 2018a)	CPU	0.90	4.11	14.1
FFDNet (Zhang et al., 2018a)	GPU	0.016	0.060	0.235
IRCNN (Zhang, Zuo, Gu et al., 2017)	CPU	0.310	1.24	4.65
IRCNN (Zhang, Zuo, Gu et al., 2017)	GPU	0.012	0.038	0.146
BRDNet (Tian, Xu, Zuo, 2020)	GPU	0.062	0.207	0.788
ADNet (Tian, Xu, Li et al., 2020)	GPU	0.0467	0.0798	0.2077
DudeNet (Tian, Xu, Zuo, Du et al., 2020)	GPU	0.018	0.422	1.246

sizes of 2784×1856 obtained by five cameras: a Nikon D800, Canon 5D Mark II, Sony A7 II, Canon 80D and Canon 600D.

4.1.2. Test datasets

The test datasets included gray-noisy and color-noisy image datasets. The gray-noisy image dataset was composed of Set12 and BSD68 (Zhang, Zuo, Chen et al., 2017). The Set12 contained 12 scenes. The BSD68 contained 68 nature images. They were used to test the Gaussian denoiser and a denoiser of blind noise. The color-noisy image dataset included CBSD68, Kodak24 (Franzen, 1999), McMaster (Zhang, Wu, Buades and Li, 2011), cc (Nam, Hwang, Matsushita, & Joo Kim, 2016), DND (Plotz & Roth, 2017), NC12 (Lebrun, Colom, & Morel, 2015), SIDD (Abdelhamed, Lin, & Brown, 2018) and Nam (Nam et al., 2016). The Kodak24 and McMaster contained 24 and 18 color noisy images, respectively. The cc contained 15 real noisy images of different ISO, i.e., 1600, 3200 and 6400. The DND contained 50 real noisy images and the clean images were captured by low-ISO images. The NC12 contained 12 noisy images and did not have ground-truth clean images. The SIDD contained real noisy images from smart phones, and consisted of 320 image pairs of noisy and ground-truth images. The Nam included 11 scenes, which were saved in JPGE format.

4.2. Experimental results

To verify the denoising performance of some methods mentioned in Section 3, we conducted some experiments on the Set12, BSD68, CBSD68, Kodak24, McMaster, DND, SIDD, Nam, cc and NC12 datasets in terms of quantitative and qualitative evaluations. The quantitative evaluation mainly used peak-signal-to-noise-ratio (PSNR) (Hore & Ziou, 2010) values of different denoisers to test the denoising effects. Additionally, we used the runtime of denoising of an image to support the PSNR for

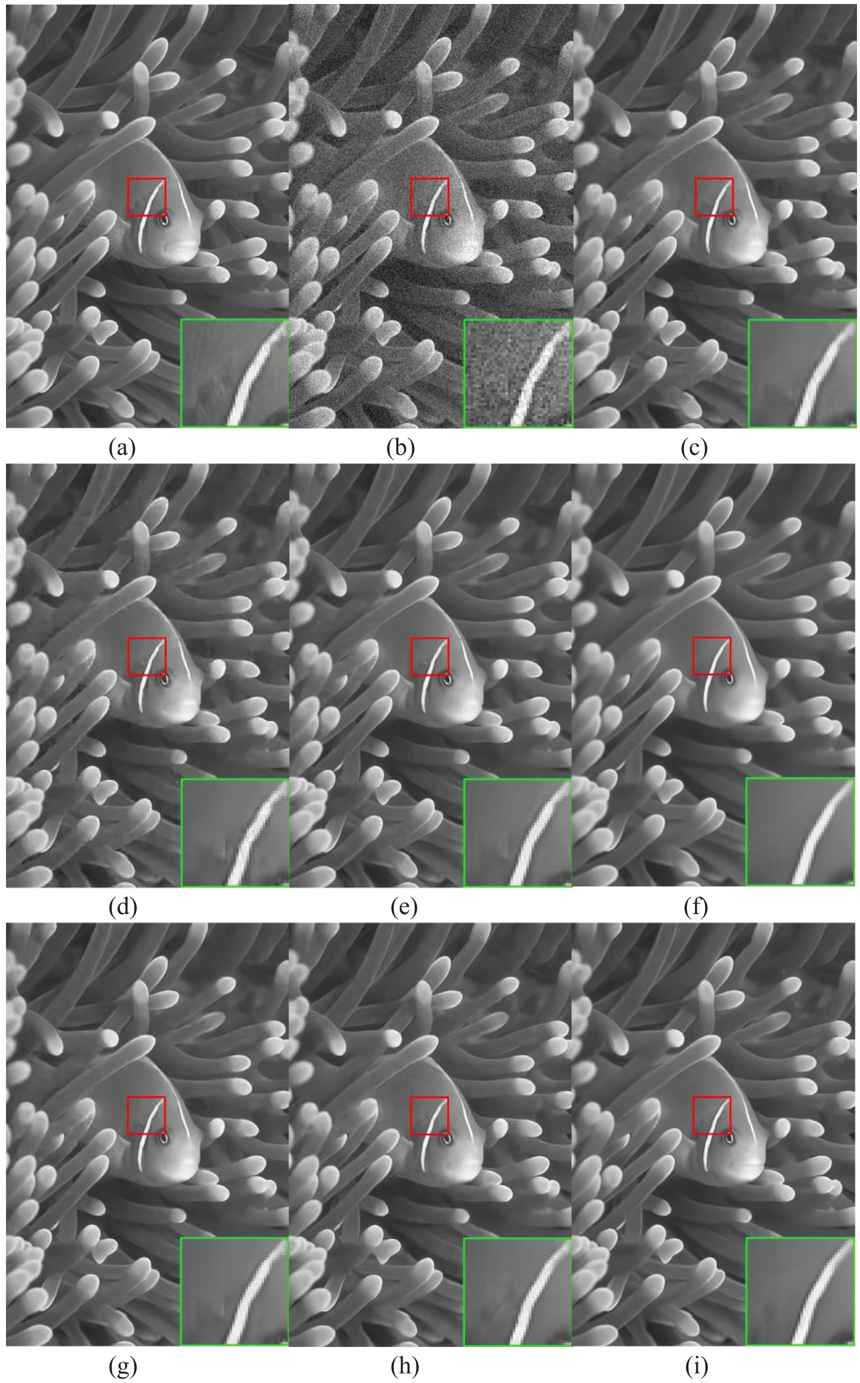

Fig. 7. Denoising results of different methods on one image from the BSD68 with $\sigma = 15$: (a) original image, (b) noisy image/24.62 dB, (c) BM3D/35.29 dB, (d) EPLL/34.98 dB, (e) DnCNN/36.20 dB, (f) FFDNet/36.75 dB, (g) IRCNN/35.94 dB, (h) ECNDNet/36.03 dB, and (i) BRDNet/36.59 dB.

quantitative evaluation. The qualitative evaluation used visual figures to show the recovered clean images.

4.2.1. Deep learning techniques for additive white noisy-image denoising

Comparisons of denoising methods should take into consideration additive white noise, including Gaussian, Poisson, low-light noise, and salt and pepper noise, all of which have significantly different noise levels. Furthermore, many of the methods use different tools, which can have a significant influence on denoising results. For these reasons, we chose typical Gaussian noise to test the denoising performance of the various methods. In addition, most of the denoising methods use PSNR as a quantitative index. Therefore, we used the BSD68, Set12, CBSD68, Kodak24 and McMaster datasets to test the denoising performance of deep learning techniques for additive white noisy-image denoising. Table 10 shows the PSNR values of different networks with different noise levels for gray additive white noisy image denoising. To understand the denoising performance of different methods, we used a feature similarity index (FSIM) (Zhang, Zhang, Mou and Zhang, 2011) as a visual quality metric to conduct experiments on BSD68 for different noise levels (i.e., 15, 25 and 50), as shown in Table 11. To test the ability of dealing with single gray additive white noisy images from different networks, Set12 was used to conduct experiments, as shown in Table 12. Table 13 displays the denoising performance of different methods for color additive

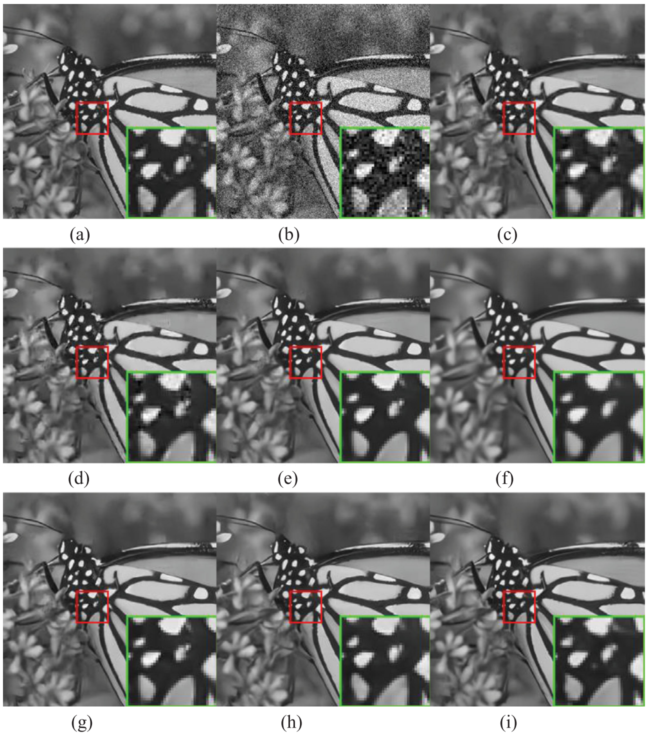

Fig. 8. Denoising results of different methods on one image from the Set12 with $\sigma = 25$: (a) original image, (b) noisy image/20.22 dB, (c) BM3D/29.26 dB, (d) EPLL/29.44 dB, (e) DnCNN/30.28 dB, (f) FFDNet/30.08 dB, (g) IRCNN/30.09 dB, (h) ECNDNet/30.30 dB, and (i) BRDNet/30.50 dB.

white noisy image denoising. Table 14 presents the efficiency of different methods for image denoising. For qualitative analysis, we magnified one area of the latent clean image from different methods. As shown in Figs. 7–10, the observed area is clearer, and the corresponding method has better denoising performance.

Table 15
PSNR (dB) of different methods on the DND for real-noisy image denoising.

Methods	DND
EPLL (Zoran & Weiss, 2011)	33.51
TNRD (Chen & Pock, 2016)	33.65
NCSR (Dong et al., 2012)	34.05
MLP (Burger et al., 2012)	34.23
BM3D (Dabov et al., 2007)	34.51
FoE (Roth & Black, 2005)	34.62
WNNM (Gu et al., 2014)	34.67
KSVD (Aharon, Elad, & Bruckstein, 2006)	36.49
CDnCNN-B (Zhang, Zuo, Chen et al., 2017)	32.43
FFDNet (Zhang et al., 2018a)	34.40
MCWNNM (Liu, Zhang et al., 2018)	37.38
TWSC (Xu, Zhang, & Zhang, 2018b)	37.94
GCBD (Chen, Chen et al., 2018)	35.58
CIMM (Anwar et al., 2017)	36.04
CBDNet (Guo et al., 2019)	37.72
VDN (Yue et al., 2019)	39.38
DRDN (Song et al., 2019)	39.40
AGAN (Lin et al., 2019)	38.13

Table 16
PSNR (dB) of different methods on the SIDD for real-noisy image denoising.

Methods	SIDD
CBM3D (Dabov et al., 2007)	25.65
WNNM (Gu et al., 2014)	25.78
MLP (Burger et al., 2012)	24.71
DnCNN-B (Zhang, Zuo, Chen et al., 2017)	23.66
CBDNet (Guo et al., 2019)	33.28
VDN (Yue et al., 2019)	39.23
DRDN (Song et al., 2019)	39.60

4.2.2. Deep learning techniques for real-noisy image denoising

For testing the denoising performance of deep learning techniques for real-noisy images, the public datasets, such as DND, SIDD, Nam and CC, were chosen to design the experiments. We chose not to use the NC12 dataset because the ground-truth clean images from NC12 were unavailable. Also, to help readers better understand these methods, we added several traditional denoising methods, such as BM3D, as comparative methods. From Tables 15 and 16, we can see that the DRDN obtained the best

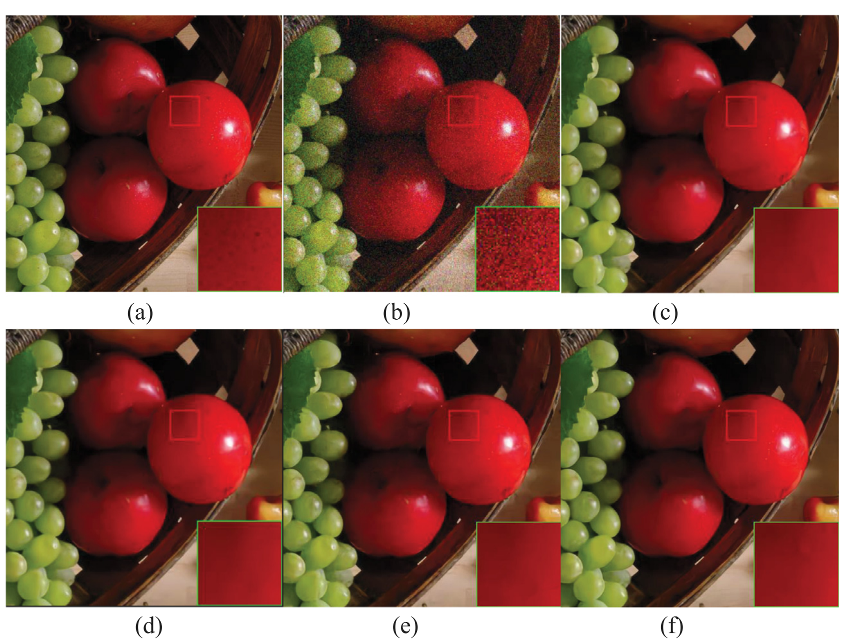

Fig. 9. Denoising results of different methods on one image from the McMaster with $\sigma = 35$: (a) original image, (b) noisy image/18.46 dB, (c) DnCNN/33.05B, (d) FFDNet/33.03 dB, (e) IRCNN/32.74 dB, and (f) BRDNet/33.26 dB.

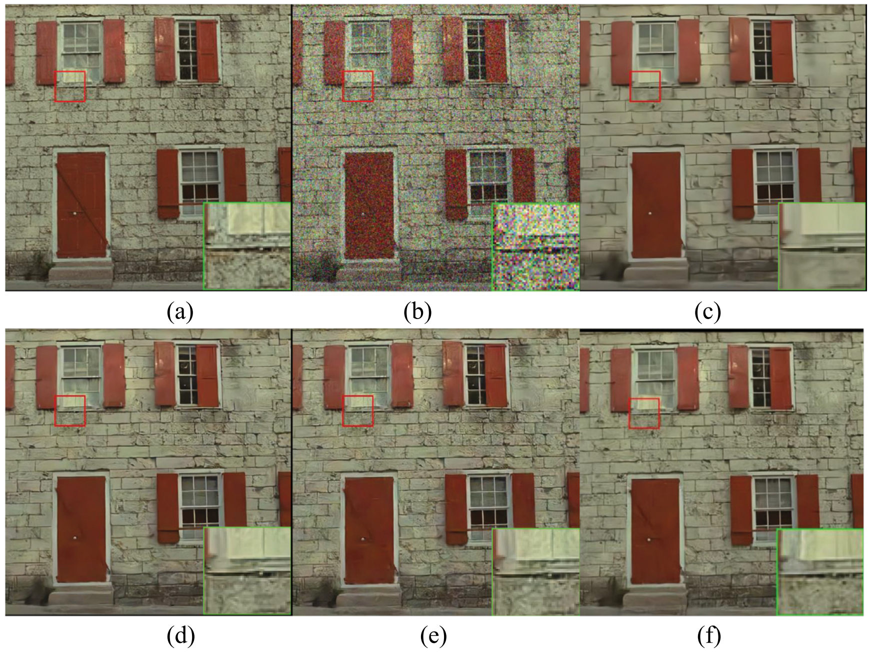

Fig. 10. Denoising results of different methods on one image from the Kodak24 with $\sigma = 50$: (a) original image, (b) noisy image/14.58 dB, (c) DnCNN/25.80B, (d) FFDNet/26.13 dB, (e) IRCNN/26.10 dB, and (f) BRDNet/26.33 dB.

Table 17
PSNR (dB) of different methods on the Nam for real-noisy image denoising.

Methods	Nam
NI (ABSoft, 2017)	31.52
TWSC (Xu et al., 2018b)	37.52
BM3D (Dabov et al., 2007)	39.84
NC (Lebrun et al., 2015)	40.41
WNNM (Gu et al., 2014)	41.04
CDnCNN-B (Zhang, Zuo, Chen et al., 2017)	37.49
MCWNNM (Liu, Zhang et al., 2018)	37.91
CBDNet (Guo et al., 2019)	41.02
CBDNet(JPEG) (Guo et al., 2019)	41.31
DRDN (Song et al., 2019)	38.45
AGAN (Lin et al., 2019)	41.38

results on the DND and SSID in real-noisy image denoising, respectively. For compressed noisy images, the AGAN obtained excellent performance, as shown in Table 17. For real noisy images of different ISO values, the SDNet and BRDNet achieved the best and second-best denoising performance, respectively, as described in Table 18.

4.2.3. Deep learning techniques for blind denoising

It is known that noise is complex in the real world, and not subject to rules. This is why blind denoising techniques, especially deep learning techniques, have been developed. Comparing the denoising performance of different deep learning techniques is very useful. The state-of-the-art denoising methods such as DnCNN, FFDNet, ADNet, SCNN and G2G1 on the BSD68 and Set12 were chosen to design the experiments. FFDNet and ADNet are superior to other methods in blind denoising, as shown in Tables 19 and 20, respectively.

4.2.4. Deep learning techniques for hybrid-noisy-image denoising

In the real world, corrupted images may include different kinds of noise (He, Dong, & Qiao, 2019), which makes it very difficult to recover a latent clean image. To resolve this problem, deep learning techniques based multi-degradation idea have been proposed, as discussed in Section 3.4. Here we introduce the denoising performance of the multi-degradation model, as shown in Table 21, where the WarpNet method is shown to be very competitive in comparison with other popular denoising methods, such as DnCNN and MemNet.

5. Discussion

Deep learning techniques are seeing increasing use in image denoising. This paper offers a survey of these techniques in order to help readers understand these methods. In this section, we present the potential areas of further research for image denoising and point out several as yet unsolved problems.

Image denoising based on deep learning techniques mainly are effective in increasing denoising performance and efficiency, and performing complex denoising tasks. Solutions for improving denoising performance include the following:

(1) Enlarging the receptive field can capture more context information. Enlarging the receptive field can be accomplished by increasing the depth and width of the networks. However, this results in higher computational costs and more memory consumption. One technique for resolving this problem, is dilated convolution, which not only contributed to higher performance and efficiency, but is also very effective for mining more edge information.

(2) The simultaneous use of extra information (also called prior knowledge) and a CNN is an effective approach to facilitate obtaining more accurate features. This is implemented by designing the loss function.

(3) Combining local and global information can enhance the memory abilities of the shallow layers on deep layers to better filter the noise. Two methods for addressing this problem are residual operation and recursive operation.

(4) Single processing methods can be used to suppress the noise. The single processing technique fused into the deep CNN can achieve excellent performance. For example, the wavelet technique is gathered into the U-Net to deal with image restoration (Liu, Zhang et al., 2018).

(5) Data augmentation, such as horizontal flip, vertical flip and color jittering, can help the denoising methods learn more

Table 18
PSNR (dB) of different methods on the cc for real-noisy image denoising.

Camera settings	CBM3D (Dabov et al., 2007)	MLP (Burger et al., 2012)	TNRD (Chen & Pock, 2016)	DnCNN (Zhang, Zuo, Chen et al., 2017)	NI (ABSoft, 2017)	NC (Lebrun et al., 2015)	WNNM (Gu et al., 2014)	BRDNet (Tian, Xu, Zuo, 2020)	SDNet (Zhao, Shao, Bao and Li, 2019)	ADNet (Tian, Xu, Li et al., 2020)	DudeNet (Tian, Xu, Zuo, Du et al., 2020)
	39.76	39.00	39.51	37.26	35.68	38.76	37.51	37.63	39.83	35.96	36.66
Canon 5D ISO = 3200	36.40	36.34	36.47	34.13	34.03	35.69	33.86	37.28	37.25	36.11	36.70
	36.37	36.33	36.45	34.09	32.63	35.54	31.43	37.75	36.79	34.49	35.03
	34.18	34.70	34.79	33.62	31.78	35.57	33.46	34.55	35.50	33.94	33.72
Nikon D600 ISO = 3200	35.07	36.20	36.37	34.48	35.16	36.70	36.09	35.99	37.24	34.33	34.70
	37.13	39.33	39.49	35.41	39.98	39.28	39.86	38.62	41.18	38.87	37.98
	36.81	37.95	38.11	35.79	34.84	38.01	36.35	39.22	38.77	37.61	38.10
Nikon D800 ISO = 1600	37.76	40.23	40.52	36.08	38.42	39.05	39.99	39.67	40.87	38.24	39.15
	37.51	37.94	38.17	35.48	35.79	38.20	37.15	39.04	38.86	36.89	36.14
	35.05	37.55	37.69	34.08	38.36	38.07	38.60	38.28	39.94	37.20	36.93
Nikon D800 ISO = 3200	34.07	35.91	35.90	33.70	35.53	35.72	36.04	37.18	36.78	35.67	35.80
	34.42	38.15	38.21	33.31	40.05	36.76	39.73	38.85	39.78	38.09	37.49
	31.13	32.69	32.81	29.83	34.08	33.49	33.29	32.75	33.34	32.24	31.94
Nikon D800 ISO = 6400	31.22	32.33	32.33	30.55	32.13	32.79	31.16	33.24	33.29	32.59	32.51
	30.97	32.29	32.29	30.09	31.52	32.86	31.98	32.89	33.22	33.14	32.91
Average	35.19	36.46	36.61	33.86	35.33	36.43	35.77	36.73	37.51	35.69	35.72

Table 19
Different methods on the BSD68 for different noise levels (i.e., 15, 25 and 50).

Methods	15	25	50
DnCNN-B (Zhang, Zuo, Chen et al., 2017)	31.61	29.16	26.23
FFDNet (Zhang et al., 2018a)	31.62	29.19	26.30
SCNN (Isogawa et al., 2017)	31.48	29.03	26.08
ADNet-B (Tian, Xu, Li et al., 2020)	31.56	29.14	26.24
DnCNN-SURE-T (Soltanayev & Chun, 2018)	–	29.00	25.95
DnCNN-MSE-GT (Soltanayev & Chun, 2018)	–	29.20	26.22
G2G1(LM,BSD) (Cha, Park, & Moon, 2019)	31.55	28.93	25.73

types of noise, which can enhance the expressive ability of the denoising models. Additionally, using the GAN to construct virtual noisy images is also useful for image denoising.

(6) Transfer learning, graph and neural architecture search methods can obtain good denoising results.

(7) Improving the hardware or camera mechanism can reduce the effect of noise on the captured image.

Compressing deep neural networks has achieved great success in improving the efficiency of denoising. Reducing the depth or the width of deep neural networks can reduce the complexity of these networks in image denoising. Also, the use of small convolutional kernel and group convolution can reduce the number of parameters, thereby accelerating the speed of training. The fusion of dimension reduction methods, such as principal component analysis (PCA) and CNN, can also lead to improvements in denoising efficiency.

For resolving complex noisy images, step-by-step processing is a very popular method. For example, using a two-step mechanism is a way of dealing with a noisy image with low-resolution. The first step involves the recovery of a high-resolution image by a CNN. The second step uses a novel CNN to filter the noise of the high-resolution image. In the example above, the two CNNs are implemented via a cascade operation. This two-step mechanism is ideal for unsupervised noise tasks, such as real noisy images and blind denoising. That is, the first step relies on a CNN with optimization algorithms, i.e., maximum a posteriori, to estimate the noise as ground truth (referred as a label). The second step utilized another CNN and obtained ground truth to train a denoising model for real-noisy image denoising or blind denoising. The self-supervised learning fused into the CNN is a good choice for real-noisy image denoising or blind denoising.

Although deep learning techniques have attained great success in these three scenarios, there are still challenges in the field of image denoising. These include:

(1) Deeper denoising networks require more memory resources.

(2) Training deeper denoising networks is not a stable solution for real noisy image, unpaired noisy image and multi-degradation tasks.

(3) Real noisy images are not easily captured, which results in inadequate training samples.

(4) Deep CNNs are difficult to solve unsupervised denoising tasks.

(5) More accurate metrics need to be found for image denoising. PSNR and SSIM are popular metrics for the task of image restoration. PSNR suffers from excessive smoothing, which is very difficult to recognize indistinguishable images. SSIM depends on brightness, contrast and structure, and therefore cannot accurately evaluate image perceptual quality.

6. Conclusion

In this paper, we compare, study and summarize the deep networks used for on image denoising. First, we show the basic frameworks of deep learning for image denoising. Then, we present the deep learning techniques for noisy tasks, including additive white noisy images, blind denoising, real noisy images and hybrid noisy images. Next, for each category of noisy tasks, we analyze the motivation and theory of denoising networks. Next, we compare the denoising results, efficiency and visual effects of different networks on benchmark datasets, and then perform a cross-comparison of the different types of image denoising methods with different types of noise. Finally, some potential areas for further research are suggested, and the challenges of deep learning in image denoising are discussed.

Table 20
Average PSNR (dB) results of different methods on Set12 with noise levels of 25 and 50.

Images	C.man	House	Peppers	Starfish	Monarch	Airplane	Parrot	Lena	Barbara	Boat	Man	Couple	Average
Noise level	$\sigma = 25$												
DnCNN-B (Zhang, Zuo, Chen et al., 2017)	29.94	33.05	30.84	29.34	30.25	29.09	29.35	32.42	29.69	30.20	30.09	30.10	30.36
FFDNet (Zhang et al., 2018a)	30.10	33.28	30.93	29.32	30.08	29.04	29.44	32.57	30.01	30.25	30.11	30.20	30.44
ADNet-B (Tian, Xu, Li et al., 2020)	29.94	33.38	30.99	29.22	30.38	29.16	29.41	32.59	30.05	30.28	30.01	30.15	30.46
DudeNet-B (Tian, Xu, Zuo, Du et al., 2020)	30.01	33.15	30.87	29.39	30.31	29.07	29.40	32.42	29.76	30.18	30.03	30.06	30.39
DNCNN-SURE-T (Soltanayev & Chun, 2018)	29.86	32.73	30.57	29.11	30.13	28.93	29.26	32.08	29.44	29.86	29.91	29.78	30.14
DNCNN-MSE-GT (Soltanayev & Chun, 2018)	30.14	33.16	30.84	29.40	30.45	29.11	29.36	32.44	29.91	30.11	30.08	30.06	30.42
Noise level	$\sigma = 50$												
DnCNN-B (Zhang, Zuo, Chen et al., 2017)	27.03	30.02	27.39	25.72	26.83	25.89	26.48	29.38	26.38	27.23	27.23	26.91	27.21
FFDNet (Zhang et al., 2018a)	27.05	30.37	27.54	25.75	26.81	25.89	26.57	29.66	26.45	27.33	27.29	27.08	27.32
ADNet-B (Tian, Xu, Li et al., 2020)	27.22	30.43	27.70	25.63	26.92	26.03	26.56	29.53	26.51	27.22	27.19	27.05	27.33
DudeNet-B (Tian, Xu, Zuo, Du et al., 2020)	27.19	30.11	27.50	25.69	26.82	25.85	26.46	29.35	26.38	27.20	27.13	26.90	27.22
DNCNN-SURE-T (Soltanayev & Chun, 2018)	26.47	29.20	26.78	25.39	26.53	25.65	26.21	28.81	25.23	26.79	26.97	26.48	26.71
DNCNN-MSE-GT (Soltanayev & Chun, 2018)	27.03	29.92	27.27	25.65	26.95	25.93	26.43	29.31	26.17	27.12	27.22	26.94	27.16

Table 21
Different methods on the VggFace2and WebFace for image denoising.

Methods	VggFace2 (Cao, Shen, Xie, Parkhi, & Zisserman, 2018)		WebFace (Yi, Lei, Liao, & Li, 2014)	
	4 ×	8 ×	4 ×	8 ×
DnCNN (Zhang, Zuo, Chen et al., 2017)	26.73	23.29	28.35	24.75
MemNet (Tai et al., 2017)	26.85	23.31	28.57	24.77
WarpNet (Li, Liu et al., 2018)	28.55	24.10	32.31	27.21

Over the past few years, Gaussian noisy image denoising techniques have achieved great success, particularly in scenarios where the Gaussian noise is regular. However, in the real world the noise is complex and irregular. Improving the hardware devices in order to better suppress the noise for capturing a high-quality image is very important. Moreover, the obtained image may be blurry, low-resolution and corrupted. Therefore, it is critical to determine how to effectively recover the latent clean image from the superposed noisy image. Furthermore, while the use of deep learning techniques to learn features requires the ground truth, the obtained real noisy images do not have the ground truth. These are urgent challenges that researches and scholars need to address.

Declaration of competing interest

The authors declare that they have no known competing financial interests or personal relationships that could have appeared to influence the work reported in this paper.

Acknowledgments

This paper is partially supported by the National Natural Science Foundation of China under Grant No. 61876051, in part by Shenzhen Municipal Science and Technology Innovation, Council under Grant No. JSGG20190220153602271 and in part by the Natural Science Foundation of Guang dong Province under Grant No. 2019A1515011811.

References

Abadi, M., Barham, P., Chen, J., Chen, Z., Davis, A., Dean, J., et al. (2016). Tensorflow: A system for large-scale machine learning. In *12th symposium on operating systems design and implementation* (pp. 265–283).

Abbasi, A., Monadjemi, A., Fang, L., Rabbani, H., & Zhang, Y. (2019). Three-dimensional optical coherence tomography image denoising through multi-input fully-convolutional networks. *Computers in Biology and Medicine*, *108*, 1–8.

Abdelhamed, A., Lin, S., & Brown, M. S. (2018). A high-quality denoising dataset for smartphone cameras. In *Proceedings of the IEEE conference on computer vision and pattern recognition* (pp. 1692–1700).

Abiko, R., & Ikehara, M. (2019). Blind denoising of mixed Gaussian-impulse noise by single cnn. In *ICASSP 2019-2019 IEEE international conference on acoustics, speech and signal processing (ICASSP)* (pp. 1717–1721). IEEE.

ABSoft, N. (2017). Neat image.

Aharon, M., Elad, M., & Bruckstein, A. (2006). K-svd: An algorithm for designing overcomplete dictionaries for sparse representation. *IEEE Transactions on Signal Processing*, *54*(11), 4311–4322.

Ahn, B., & Cho, N. I. (2017). Block-matching convolutional neural network for image denoising. arXiv preprint arXiv:1704.00524.

Ahn, B., Kim, Y., Park, G., & Cho, N. I. (2018). Block-matching convolutional neural network (bmcnn): Improving cnn-based denoising by block-matched inputs. In *2018 Asia-Pacific signal and information processing association annual summit and conference (APSIPA ASC)* (pp. 516–525). IEEE.

Aittala, M., & Durand, F. (2018). Burst image deblurring using permutation invariant convolutional neural networks. In *Proceedings of the European conference on computer vision (ECCV)* (pp. 731–747).

Aljadaany, R., Pal, D. K., & Savvides, M. (2019). Proximal splitting networks for image restoration. arXiv preprint arXiv:1903.07154.

Anwar, S., & Barnes, N. (2019). Real image denoising with feature attention. arXiv preprint arXiv:1904.07396.

Anwar, S., Huynh, C. P., & Porikli, F. (2017). Chaining identity mapping modules for image denoising. arXiv preprint arXiv:1712.02933.

Bae, W., Yoo, J., & Chul Ye, J. (2017). Beyond deep residual learning for image restoration: Persistent homology-guided manifold simplification. In *Proceedings of the IEEE conference on computer vision and pattern recognition workshops* (pp. 145–153).

Bako, S., Vogels, T., McWilliams, B., Meyer, M., Novák, J., Harvill, A., et al. (2017). Kernel-predicting convolutional networks for denoising Monte Carlo renderings. *ACM Transactions on Graphics*, *36*(4), 97.

Bedini, L., & Tonazzini, A. (1990). Neural network use in maximum entropy image restoration. *Image and Vision Computing*, *8*(2), 108–114.

Bedini, L., & Tonazzini, A. (1992). Image restoration preserving discontinuities: the bayesian approach and neural networks. *Image and Vision Computing*, *10*(2), 108–118.

Bengio, Y., Lamblin, P., Popovici, D., & Larochelle, H. (2007). Greedy layer-wise training of deep networks. In *Advances in neural information processing systems* (pp. 153–160).

Bergstra, J., Breuleux, O., Bastien, F., Lamblin, P., Pascanu, R., Desjardins, G., et al. (2010). Theano: a cpu and gpu math expression compiler. In *Proceedings of the python for scientific computing conference (SciPy), Vol. 4* Austin, TX.

Bernstein, R. (1987). Adaptive nonlinear filters for simultaneous removal of different kinds of noise in images. *IEEE Transactions on Circuits and Systems*, *34*(11), 1275–1291.

Bigdeli, S. A., & Zwicker, M. (2017). Image restoration using autoencoding priors. arXiv preprint arXiv:1703.09964.

Bigdeli, S. A., Zwicker, M., Favaro, P., & Jin, M. (2017). Deep mean-shift priors for image restoration. In *Advances in neural information processing systems* (pp. 763–772).

Bottou, L. (2010). Large-scale machine learning with stochastic gradient descent. In *Proceedings of COMPSTAT'2010* (pp. 177–186). Springer.

Broaddus, C., Krull, A., Weigert, M., Schmidt, U., & Myers, G. (2020). Removing structured noise with self-supervised blind-spot networks. In *2020 IEEE 17th international symposium on biomedical imaging (ISBI)* (pp. 159–163). IEEE.

Brooks, T., Mildenhall, B., Xue, T., Chen, J., Sharlet, D., & Barron, J. T. (2019). Unprocessing images for learned raw denoising. In *Proceedings of the IEEE conference on computer vision and pattern recognition* (pp. 11036–11045).

Burger, H. C., Schuler, C. J., & Harmeling, S. (2012). Image denoising: Can plain neural networks compete with bm3d?. In *2012 IEEE conference on computer vision and pattern recognition* (pp. 2392–2399). IEEE.

Cao, Q., Shen, L., Xie, W., Parkhi, O. M., & Zisserman, A. (2018). Vggface2: A dataset for recognising faces across pose and age. In *2018 13th IEEE international conference on automatic face & gesture recognition (FG 2018)* (pp. 67–74). IEEE.

Cha, S., Park, T., & Moon, T. (2019). Gan2gan: Generative noise learning for blind image denoising with single noisy images. arXiv preprint arXiv:1905.10488.

Chang, Y., Yan, L., Fang, H., Zhong, S., & Liao, W. (2018). Hsi-denet: Hyperspectral image restoration via convolutional neural network. *IEEE Transactions on Geoscience and Remote Sensing*, *57*(2), 667–682.

Chen, J., Chen, J., Chao, H., & Yang, M. (2018). Image blind denoising with generative adversarial network based noise modeling. In *Proceedings of the IEEE conference on computer vision and pattern recognition* (pp. 3155–3164).

Chen, J., Hou, J., & Chau, L.-P. (2018). Light field denoising via anisotropic parallax analysis in a cnn framework. *IEEE Signal Processing Letters*, *25*(9), 1403–1407.

Chen, Y., & Pock, T. (2016). Trainable nonlinear reaction diffusion: A flexible framework for fast and effective image restoration. *IEEE Transactions on Pattern Analysis and Machine Intelligence*, *39*(6), 1256–1272.

Chen, X., Song, L., & Yang, X. (2016). Deep rnns for video denoising. In *Applications of digital image processing XXXIX, Vol. 9971* (p. 99711T). International Society for Optics and Photonics.

Chen, C., Xiong, Z., Tian, X., & Wu, F. (2018). Deep boosting for image denoising. In *Proceedings of the European conference on computer vision (ECCV)* (pp. 3–18).

Chen, C., & Xu, Z. (2018). Aerial-image denoising based on convolutional neural network with multi-scale residual learning approach. *Information*, *9*(7), 169.

Chen, Y., Yu, M., Jiang, G., Peng, Z., & Chen, F. (2019). End-to-end single image enhancement based on a dual network cascade model. *Journal of Visual Communication and Image Representation*, *61*, 284–295.

Chen, X., Zhan, S., Ji, D., Xu, L., Wu, C., & Li, X. (2018). Image denoising via deep network based on edge enhancement. *Journal of Ambient Intelligence and Humanized Computing*, 1–11.

Chetlur, S., Woolley, C., Vandermersch, P., Cohen, J., Tran, J., Catanzaro, B., et al. (2014). Cudnn: Efficient primitives for deep learning. arXiv preprint arXiv:1410.0759.

Chiang, Y.-W., & Sullivan, B. (1989). Multi-frame image restoration using a neural network. In *Proceedings of the 32nd midwest symposium on circuits and systems,* (pp. 744–747). IEEE.

Cho, S. I., & Kang, S.-J. (2018). Gradient prior-aided cnn denoiser with separable convolution-based optimization of feature dimension. *IEEE Transactions on Multimedia*, *21*(2), 484–493.

Choi, K., Vania, M., & Kim, S. (2019). Semi-supervised learning for low-dose ct image restoration with hierarchical deep generative adversarial network (hd-gan). In *2019 41st annual international conference of the IEEE engineering in medicine and biology society (EMBC)* (pp. 2683–2686). IEEE.

Chollet, F., et al. (2015). Keras.

Couturier, R., Perrot, G., & Salomon, M. (2018). Image denoising using a deep encoder-decoder network with skip connections. In *International conference on neural information processing* (pp. 554–565). Springer.

Cruz, C., Foi, A., Katkovnik, V., & Egiazarian, K. (2018). Nonlocality-reinforced convolutional neural networks for image denoising. *IEEE Signal Processing Letters*, *25*(8), 1216–1220.

Cui, J., Gong, K., Guo, N., Wu, C., Meng, X., Kim, K., et al. (2019). Pet image denoising using unsupervised deep learning. *European Journal of Nuclear Medicine and Molecular Imaging*, *46*(13), 2780–2789.

Dabov, K., Foi, A., Katkovnik, V., & Egiazarian, K. (2007). Image denoising by sparse 3-d transform-domain collaborative filtering. *IEEE Transactions on Image Processing*, *16*(8), 2080–2095.

Davy, A., Ehret, T., Morel, J.-M., Arias, P., & Facciolo, G. (2018). Non-local video denoising by cnn. arXiv preprint arXiv:1811.12758.

Dong, W., Zhang, L., Shi, G., & Li, X. (2012). Nonlocally centralized sparse representation for image restoration. *IEEE Transactions on Image Processing*, *22*(4), 1620–1630.

Du, H., Dong, L., Liu, M., Zhao, Y., Jia, W., Liu, X., et al. (2018). Image restoration based on deep convolutional network in wavefront coding imaging system. In *2018 digital image computing: techniques and applications (DICTA)* (pp. 1–8). IEEE.

Du, B., Wei, Q., & Liu, R. (2019). An improved quantum-behaved particle swarm optimization for endmember extraction. *IEEE Transactions on Geoscience and Remote Sensing*.

Duan, C., Cui, L., Chen, X., Wei, F., Zhu, C., & Zhao, T. (2018). Attention-fused deep matching network for natural language inference.. In *IJCAI* (pp. 4033–4040).

Ehret, T., Davy, A., Morel, J.-M., Facciolo, G., & Arias, P. (2019). Model-blind video denoising via frame-to-frame training. In *Proceedings of the IEEE conference on computer vision and pattern recognition* (pp. 11369–11378).

Elad, M., & Aharon, M. (2006). Image denoising via sparse and redundant representations over learned dictionaries. *IEEE Transactions on Image Processing*, *15*(12), 3736–3745.

Fan, E. (2000). Extended tanh-function method and its applications to nonlinear equations. *Physics Letters. A*, *277*(4–5), 212–218.

Farooque, M. A., & Rohankar, J. S. (2013). Survey on various noises and techniques for denoising the color image. *International Journal of Application or Innovation in Engineering & Management (IJAIEM)*, *2*(11), 217–221.

de Figueiredo, M. T., & Leitao, J. M. (1992). Image restoration using neural networks. In *[Proceedings] ICASSP-92: 1992 IEEE international conference on acoustics, speech, and signal processing, Vol. 2* (pp. 409–412). IEEE.

Franzen, R. (1999). Kodak lossless true color image suite. source: http://r0k.us/graphics/kodak 4.

Fu, B., Zhao, X., Li, Y., Wang, X., & Ren, Y. (2019). A convolutional neural networks denoising approach for salt and pepper noise. *Multimedia Tools and Applications*, *78*(21), 30707–30721.

Fukushima, K. (1980). Neocognitron: A self-organizing neural network model for a mechanism of pattern recognition unaffected by shift in position. *Biological Cybernetics*, *36*(4), 193–202.

Fukushima, K., & Miyake, S. (1982). Neocognitron: A self-organizing neural network model for a mechanism of visual pattern recognition. In *Competition and cooperation in neural nets* (pp. 267–285). Springer.

Gardner, E., Wallace, D., & Stroud, N. (1989). Training with noise and the storage of correlated patterns in a neural network model. *Journal of Physics A: Mathematical and General*, *22*(12), 2019.

Gashi, D., Pereira, M., & Vterkovska, V. (2017). Multi-scale context aggregation by dilated convolutions machine learning-project.

Gholizadeh-Ansari, M., Alirezaie, J., & Babyn, P. (2018). Low-dose ct denoising with dilated residual network. In *2018 40th annual international conference of the IEEE engineering in medicine and biology society (EMBC)* (pp. 5117–5120). IEEE.

Godard, C., Matzen, K., & Uyttendaele, M. (2018). Deep burst denoising. In *Proceedings of the European conference on computer vision (ECCV)* (pp. 538–554).

Gondara, L., & Wang, K. (2017). Recovering loss to followup information using denoising autoencoders. In *2017 IEEE international conference on big data (Big Data)* (pp. 1936–1945). IEEE.

Gong, D., Zhang, Z., Shi, Q., Hengel, A. v. d., Shen, C., & Zhang, Y. (2018). Learning an optimizer for image deconvolution. arXiv preprint arXiv:1804.03368.

Green, M., Marom, E. M., Konen, E., Kiryati, N., & Mayer, A. (2018). Learning real noise for ultra-low dose lung ct denoising. In *International workshop on patch-based techniques in medical imaging* (pp. 3–11). Springer.

Greenhill, D., & Davies, E. (1994). Relative effectiveness of neural networks for image noise suppression. In *Machine intelligence and pattern recognition, Vol. 16* (pp. 367–378). Elsevier.

Gu, S., Zhang, L., Zuo, W., & Feng, X. (2014). Weighted nuclear norm minimization with application to image denoising. In *Proceedings of the IEEE conference on computer vision and pattern recognition* (pp. 2862–2869).

Guan, J., Lai, R., & Xiong, A. (2019). Wavelet deep neural network for stripe noise removal. *IEEE Access*, *7*, 44544–44554.

Guo, Z., Sun, Y., Jian, M., & Zhang, X. (2018). Deep residual network with sparse feedback for image restoration. *Applied Sciences*, *8*(12), 2417.

Guo, S., Yan, Z., Zhang, K., Zuo, W., & Zhang, L. (2019). Toward convolutional blind denoising of real photographs. In *Proceedings of the IEEE conference on computer vision and pattern recognition* (pp. 1712–1722).

Han, Y., & Ye, J. C. (2018). Framing u-net via deep convolutional framelets: Application to sparse-view ct. *IEEE Transactions on Medical Imaging*, *37*(6), 1418–1429.

He, J., Dong, C., & Qiao, Y. (2019). Multi-dimension modulation for image restoration with dynamic controllable residual learning. arXiv preprint arXiv:1912.05293.

He, K., Zhang, X., Ren, S., & Sun, J. (2016). Deep residual learning for image recognition. In *Proceedings of the IEEE conference on computer vision and pattern recognition* (pp. 770–778).

Heckel, R., Huang, W., Hand, P., & Voroninski, V. (2018). Rate-optimal denoising with deep neural networks. arXiv preprint arXiv:1805.08855.

Heinrich, M. P., Stille, M., & Buzug, T. M. (2018). Residual u-net convolutional neural network architecture for low-dose ct denoising. *Current Directions in Biomedical Engineering*, *4*(1), 297–300.

Hendriksen, A. A., Pelt, D. M., & Batenburg, K. J. (2020). Noise2inverse: Self-supervised deep convolutional denoising for linear inverse problems in imaging. arXiv preprint arXiv:2001.11801.

Hinton, G., & Osindero, S. (2006). The, y. 2006. a fast learning algorithm for deep belief nets. *Neural Computation*, *18*(7).

Hinton, G. E., & Salakhutdinov, R. R. (2006). Reducing the dimensionality of data with neural networks. *Science*, *313*(5786), 504–507.

Hirose, Y., Yamashita, K., & Hijiya, S. (1991). Back-propagation algorithm which varies the number of hidden units. *Neural Networks*, *4*(1), 61–66.

Hong, S.-W., & Bao, P. (2000). An edge-preserving subband coding model based on non-adaptive and adaptive regularization. *Image and Vision Computing*, *18*(8), 573–582.

Hongqiang, M., Shiping, M., Yuelei, X., & Mingming, Z. (2018). An adaptive image denoising method based on deep rectified denoising auto-encoder. *Journal of Physics: Conference Series*, *1060*(1), Article 012048, IOP Publishing.

Hore, A., & Ziou, D. (2010). Image quality metrics: psnr vs. ssim. In *2010 20th international conference on pattern recognition* (pp. 2366–2369). IEEE.

Hsu, C.-C., & Lin, C.-W. (2017). Cnn-based joint clustering and representation learning with feature drift compensation for large-scale image data. *IEEE Transactions on Multimedia*, *20*(2), 421–429.

Hu, G., Yang, Y., Yi, D., Kittler, J., Christmas, W., Li, S. Z., et al. (2015). When face recognition meets with deep learning: an evaluation of convolutional neural networks for face recognition. In *Proceedings of the IEEE international conference on computer vision workshops* (pp. 142–150).

Huang, T. (1971). Stability of two-dimensional recursive filters(mathematical model for stability problem in two-dimensional recursive filtering).

Ioffe, S. (2017). Batch renormalization: Towards reducing minibatch dependence in batch-normalized models. In *Advances in neural information processing systems* (pp. 1945–1953).

Ioffe, S., & Szegedy, C. (2015). Batch normalization: Accelerating deep network training by reducing internal covariate shift. arXiv preprint arXiv:1502.03167.

Isogawa, K., Ida, T., Shiodera, T., & Takeguchi, T. (2017). Deep shrinkage convolutional neural network for adaptive noise reduction. *IEEE Signal Processing Letters*, *25*(2), 224–228.

Jaroensri, R., Biscarrat, C., Aittala, M., & Durand, F. (2019). Generating training data for denoising real RGB images via camera pipeline simulation. arXiv preprint arXiv:1904.08825.

Jarrett, K., Kavukcuoglu, K., Ranzato, M., & LeCun, Y. (2009). What is the best multi-stage architecture for object recognition?. In *2009 IEEE 12th international conference on computer vision* (pp. 2146–2153). IEEE.

Jeon, W., Jeong, W., Son, K., & Yang, H. (2018). Speckle noise reduction for digital holographic images using multi-scale convolutional neural networks. *Optics Letters*, *43*(17), 4240–4243.

Jia, X., Chai, H., Guo, Y., Huang, Y., & Zhao, B. (2018). Multiscale parallel feature extraction convolution neural network for image denoising. *Journal of Electronic Imaging*, *27*(6), Article 063031.

Jia, X., Liu, S., Feng, X., & Zhang, L. (2019). FOCNet: A fractional optimal control network for image denoising. In *Proceedings of the IEEE conference on computer vision and pattern recognition* (pp. 6054–6063).

Jia, Y., Shelhamer, E., Donahue, J., Karayev, S., Long, J., Girshick, R., et al. (2014). Caffe: Convolutional architecture for fast feature embedding. In *Proceedings of the 22nd ACM international conference on multimedia* (pp. 675–678). ACM.

Jian, W., Zhao, H., Bai, Z., & Fan, X. (2018). Low-light remote sensing images enhancement algorithm based on fully convolutional neural network. In *China high resolution earth observation conference* (pp. 56–65). Springer.

Jiang, D., Dou, W., Vosters, L., Xu, X., Sun, Y., & Tan, T. (2018). Denoising of 3D magnetic resonance images with multi-channel residual learning of convolutional neural network. *Japanese Journal of Radiology*, *36*(9), 566–574.

Jiang, L., Jing, Y., Hu, S., Ge, B., & Xiao, W. (2018). Deep refinement network for natural low-light image enhancement in symmetric pathways. *Symmetry*, *10*(10), 491.

Jiao, J., Tu, W.-C., He, S., & Lau, R. W. (2017). Formresnet: Formatted residual learning for image restoration. In *Proceedings of the IEEE conference on computer vision and pattern recognition workshops* (pp. 38–46).

Jifara, W., Jiang, F., Rho, S., Cheng, M., & Liu, S. (2019). Medical image denoising using convolutional neural network: a residual learning approach. *The Journal of Supercomputing*, *75*(2), 704–718.

Jin, K. H., McCann, M. T., Froustey, E., & Unser, M. (2017). Deep convolutional neural network for inverse problems in imaging. *IEEE Transactions on Image Processing*, *26*(9), 4509–4522.

Kadimesetty, V. S., Gutta, S., Ganapathy, S., & Yalavarthy, P. K. (2018). Convolutional neural network-based robust denoising of low-dose computed tomography perfusion maps. *IEEE Transactions on Radiation and Plasma Medical Sciences*, *3*(2), 137–152.

Karlik, B., & Olgac, A. V. (2011). Performance analysis of various activation functions in generalized mlp architectures of neural networks. *International Journal of Artificial Intelligence and Expert Systems*, *1*(4), 111–122.

Khan, S., Khan, K. S., & Shin, S. Y. (2019). Symbol denoising in high order m-QAM using residual learning of deep cnn. In *2019 16th IEEE annual consumer communications & networking conference (CCNC)* (pp. 1–6). IEEE.

Khaw, H. Y., Soon, F. C., Chuah, J. H., & Chow, C.-O. (2017). Image noise types recognition using convolutional neural network with principal components analysis. *IET Image Processing*, *11*(12), 1238–1245.

Khoroushadi, M., & Sadegh, M. (2018). *Enhancement in Low-dose computed tomography through image denoising techniques: Wavelets and deep learning* (Ph.D. thesis), ProQuest Dissertations Publishing.

Kokkinos, F., & Lefkimmiatis, S. (2019). Iterative joint image demosaicking and denoising using a residual denoising network. *IEEE Transactions on Image Processing*.

Krizhevsky, A., Sutskever, I., & Hinton, G. E. (2012). Imagenet classification with deep convolutional neural networks. In *Advances in neural information processing systems* (pp. 1097–1105).

Kutzner, C., Páll, S., Fechner, M., Esztermann, A., de Groot, B. L., & Grubmüller, H. (2019). More bang for your buck: improved use of GPU nodes for GROMACS 2018. arXiv preprint arXiv:1903.05918.

Latif, G., Iskandar, D. A., Alghazo, J., Butt, M., & Khan, A. H. (2018). Deep cnn based mr image denoising for tumor segmentation using watershed transform. *International Journal of Engineering & Technology*, *7*(2.3), 37–42.

Lebrun, M., Colom, M., & Morel, J.-M. (2015). The noise clinic: a blind image denoising algorithm. *Image Processing On Line*, *5*, 1–54.

LeCun, Y., Bottou, L., Bengio, Y., Haffner, P., et al. (1998). Gradient-based learning applied to document recognition. *Proceedings of the IEEE*, *86*(11), 2278–2324.

Lee, C.-C., & de Gyvez, J. P. (1996). Color image processing in a cellular neural-network environment. *IEEE Transactions on Neural Networks*, *7*(5), 1086–1098.

Lee, D., Yun, S., Choi, S., Yoo, H., Yang, M.-H., & Oh, S. (2018). Unsupervised holistic image generation from key local patches. In *Proceedings of the European conference on computer vision (ECCV)* (pp. 19–35).

Lefkimmiatis, S. (2017). Non-local color image denoising with convolutional neural networks. In *Proceedings of the IEEE conference on computer vision and pattern recognition* (pp. 3587–3596).

Lei, Y., Yuan, W., Wang, H., Wenhu, Y., & Bo, W. (2016). A skin segmentation algorithm based on stacked autoencoders. *IEEE Transactions on Multimedia*, *19*(4), 740–749.

Li, Q., Cai, W., Wang, X., Zhou, Y., Feng, D. D., & Chen, M. (2014). Medical image classification with convolutional neural network. In *2014 13th international conference on control automation robotics & vision (ICARCV)* (pp. 844–848). IEEE.

Li, X., Du, B., Xu, C., Zhang, Y., Zhang, L., & Tao, D. (2020). Robust learning with imperfect privileged information. *Artificial Intelligence*, *282*, Article 103246.

Li, S., He, F., Du, B., Zhang, L., Xu, Y., & Tao, D. (2019). Fast spatio-temporal residual network for video super-resolution. arXiv preprint arXiv:1904.02870.

Li, M., Hsu, W., Xie, X., Cong, J., & Gao, W. (2020). Sacnn: Self-attention convolutional neural network for low-dose ct denoising with self-supervised perceptual loss network. *IEEE Transactions on Medical Imaging*.

Li, J., Li, M., Lu, G., Zhang, B., Yin, H., & Zhang, D. (2020). Similarity and diversity induced paired projection for cross-modal retrieval. *Information Sciences*.

Li, X., Liu, M., Ye, Y., Zuo, W., Lin, L., & Yang, R. (2018). Learning warped guidance for blind face restoration. In *Proceedings of the European conference on computer vision (ECCV)* (pp. 272–289).

Li, J., Lu, G., Zhang, B., You, J., & Zhang, D. (2019). Shared linear encoder-based multikernel gaussian process latent variable model for visual classification. *IEEE Transactions on Cybernetics*.

Li, Z., & Wu, J. (2019). Learning deep cnn denoiser priors for depth image inpainting. *Applied Sciences*, *9*(6), 1103.

Li, L., Wu, J., & Jin, X. (2018). Cnn denoising for medical image based on wavelet domain. In *2018 9th international conference on information technology in medicine and education (ITME)* (pp. 105–109). IEEE.

Li, H., Yang, W., & Yong, X. (2018). Deep learning for ground-roll noise attenuation. In *SEG technical program expanded abstracts 2018* (pp. 1981–1985). Society of Exploration Geophysicists.

Li, J., Zhang, B., & Zhang, D. (2017). Shared autoencoder gaussian process latent variable model for visual classification. *IEEE Transactions on Neural Networks and Learning Systems*, *29*(9), 4272–4286.

Liang, J., & Liu, R. (2015). Stacked denoising autoencoder and dropout together to prevent overfitting in deep neural network. In *2015 8th international congress on image and signal processing (CISP)* (pp. 697–701). IEEE.

Liang, X., Zhang, D., Lu, G., Guo, Z., & Luo, N. (2019). A novel multicamera system for high-speed touchless palm recognition. *IEEE Transactions on Systems, Man, and Cybernetics: Systems*.

Lin, M., Chen, Q., & Yan, S. (2013). Network in network. arXiv preprint arXiv:1312.4400.

Lin, K., Li, T. H., Liu, S., & Li, G. (2019). Real photographs denoising with noise domain adaptation and attentive generative adversarial network. In *Proceedings of the IEEE conference on computer vision and pattern recognition workshops* (pp. 0–0).

Litjens, G., Kooi, T., Bejnordi, B. E., Setio, A. A. A., Ciompi, F., Ghafoorian, M., et al. (2017). A survey on deep learning in medical image analysis. *Medical Image Analysis*, *42*, 60–88.

Liu, P., & Fang, R. (2017). Wide inference network for image denoising via learning pixel-distribution prior. arXiv preprint arXiv:1707.05414.

Liu, W., & Lee, J. (2019). A 3-d atrous convolution neural network for hyperspectral image denoising. *IEEE Transactions on Geoscience and Remote Sensing*.

Liu, P., Li, Y., El Basha, M. D., & Fang, R. (2018). Neural network evolution using expedited genetic algorithm for medical image denoising. In *International conference on medical image computing and computer-assisted intervention* (pp. 12–20). Springer.

Liu, Q., Lu, X., He, Z., Zhang, C., & Chen, W.-S. (2017). Deep convolutional neural networks for thermal infrared object tracking. *Knowledge-Based Systems*, *134*, 189–198.

Liu, X., Suganuma, M., Sun, Z., & Okatani, T. (2019). Dual residual networks leveraging the potential of paired operations for image restoration. In *Proceedings of the IEEE conference on computer vision and pattern recognition* (pp. 7007–7016).

Liu, D., Wen, B., Liu, X., Wang, Z., & Huang, T. S. (2017). When image denoising meets high-level vision tasks: A deep learning approach. arXiv preprint arXiv:1706.04284.

Liu, P., Zhang, H., Zhang, K., Lin, L., & Zuo, W. (2018). Multi-level wavelet-cnn for image restoration. In *Proceedings of the IEEE conference on computer vision and pattern recognition workshops* (pp. 773–782).

Lo, S.-C., Lou, S.-L., Lin, J.-S., Freedman, M. T., Chien, M. V., & Mun, S. K. (1995). Artificial convolution neural network techniques and applications for lung nodule detection. *IEEE Transactions on Medical Imaging*, *14*(4), 711–718.

Loo Tiang Kuan, L. (2017). *Survey of deep neural networks in blind denoising using different architectures and different labels* (Ph.D. thesis).

Lu, Y., Lai, Z., Li, X., Wong, W. K., Yuan, C., & Zhang, D. (2018). Low-rank 2-d neighborhood preserving projection for enhanced robust image representation. *IEEE Transactions on Cybernetics*, *49*(5), 1859–1872.

Lu, Y., Wong, W., Lai, Z., & Li, X. (2019). Robust flexible preserving embedding.. *IEEE Transactions on Cybernetics*.

Lu, Z., Yu, Z., Ya-Li, P., Shi-Gang, L., Xiaojun, W., Gang, L., et al. (2018). Fast single image super-resolution via dilated residual networks. *IEEE Access*.

Lucas, A., Iliadis, M., Molina, R., & Katsaggelos, A. K. (2018). Using deep neural networks for inverse problems in imaging: beyond analytical methods. *IEEE Signal Processing Magazine*, *35*(1), 20–36.

Ma, Y., Chen, X., Zhu, W., Cheng, X., Xiang, D., & Shi, F. (2018). Speckle noise reduction in optical coherence tomography images based on edge-sensitive cgan. *Biomedical Optics Express*, *9*(11), 5129–5146.

Ma, K., Duanmu, Z., Wu, Q., Wang, Z., Yong, H., Li, H., et al. (2016). Waterloo exploration database: New challenges for image quality assessment models. *IEEE Transactions on Image Processing*, *26*(2), 1004–1016.

Mafi, M., Martin, H., Cabrerizo, M., Andrian, J., Barreto, A., & Adjouadi, M. (2018). A comprehensive survey on impulse and Gaussian denoising filters for digital images. *Signal Processing*.

Mairal, J., Bach, F. R., Ponce, J., Sapiro, G., & Zisserman, A. (2009). Non-local sparse models for image restoration.. In *ICCV, Vol. 29* (pp. 54–62). Citeseer.

Majumdar, A. (2018). Blind denoising autoencoder. *IEEE Transactions on Neural Networks and Learning Systems*, *30*(1), 312–317.

Mao, X., Shen, C., & Yang, Y.-B. (2016). Image restoration using very deep convolutional encoder-decoder networks with symmetric skip connections. In *Advances in neural information processing systems* (pp. 2802–2810).

Marinč, T., Srinivasan, V., Gül, S., Hellge, C., & Samek, W. (2019). Multi-kernel prediction networks for denoising of burst images. In *2019 IEEE international conference on image processing (ICIP)* (pp. 2404–2408). IEEE.

Marreiros, A. C., Daunizeau, J., Kiebel, S. J., & Friston, K. J. (2008). Population dynamics: variance and the sigmoid activation function. *Neuroimage*, *42*(1), 147–157.

McCann, M. T., Jin, K. H., & Unser, M. (2017). Convolutional neural networks for inverse problems in imaging: A review. *IEEE Signal Processing Magazine*, *34*(6), 85–95.

Meinhardt, T., Moller, M., Hazirbas, C., & Cremers, D. (2017). Learning proximal operators: Using denoising networks for regularizing inverse imaging problems. In *Proceedings of the IEEE international conference on computer vision* (pp. 1781–1790).

Meng, M., Li, S., Yao, L., Li, D., Zhu, M., Gao, Q., et al. (2020). Semi-supervised learned sinogram restoration network for low-dose ct image reconstruction. In *Medical imaging 2020: Physics of medical imaging, Vol. 11312* (p. 113120B). International Society for Optics and Photonics.

Mildenhall, B., Barron, J. T., Chen, J., Sharlet, D., Ng, R., & Carroll, R. (2018). Burst denoising with kernel prediction networks. In *Proceedings of the IEEE conference on computer vision and pattern recognition* (pp. 2502–2510).

Nair, V., & Hinton, G. E. (2010). Rectified linear units improve restricted boltzmann machines. In *Proceedings of the 27th international conference on machine learning (ICML-10)* (pp. 807–814).

Nam, S., Hwang, Y., Matsushita, Y., & Joo Kim, S. (2016). A holistic approach to cross-channel image noise modeling and its application to image denoising. In *Proceedings of the IEEE conference on computer vision and pattern recognition* (pp. 1683–1691).

Nossek, J., & Roska, T. (1993). Special issue on cellular neural networks-introduction.

Nvidia, C. (2011). Nvidia cuda c programming guide. *Nvidia Corporation*, *120*(18), 8.

Osher, S., Burger, M., Goldfarb, D., Xu, J., & Yin, W. (2005). An iterative regularization method for total variation-based image restoration. *Multiscale Modeling and Simulation*, *4*(2), 460–489.

Paik, J. K., & Katsaggelos, A. K. (1992). Image restoration using a modified hopfield network. *IEEE Transactions on Image Processing*, *1*(1), 49–63.

Panda, A., Naskar, R., & Pal, S. (2018). Exponential linear unit dilated residual network for digital image denoising. *Journal of Electronic Imaging*, *27*(5), Article 053024.

Pardasani, R., & Shreemali, U. (2018). Image denoising and super-resolution using residual learning of deep convolutional network. arXiv preprint arXiv:1809.08229.

Park, J. H., Kim, J. H., & Cho, S. I. (2018). The analysis of cnn structure for image denoising. In *2018 international SoC design conference (ISOCC)* (pp. 220–221). IEEE.

Paszke, A., Gross, S., Chintala, S., Chanan, G., Yang, E., DeVito, Z., et al. (2017). Automatic differentiation in pytorch.

Peng, Y., Zhang, L., Liu, S., Wu, X., Zhang, Y., & Wang, X. (2019). Dilated residual networks with symmetric skip connection for image denoising. *Neurocomputing*, *345*, 67–76.

Pitas, I., & Venetsanopoulos, A. (1986). Nonlinear mean filters in image processing. *IEEE Transactions on Acoustics, Speech and Signal Processing*, *34*(3), 573–584.

Plotz, T., & Roth, S. (2017). Benchmarking denoising algorithms with real photographs. In *Proceedings of the IEEE conference on computer vision and pattern recognition* (pp. 1586–1595).

Priyanka, S. A., & Wang, Y.-K. (2019). Fully symmetric convolutional network for effective image denoising. *Applied Sciences*, *9*(4), 778.

Radford, A., Metz, L., & Chintala, S. (2015). Unsupervised representation learning with deep convolutional generative adversarial networks. arXiv preprint arXiv:1511.06434.

Ran, M., Hu, J., Chen, Y., Chen, H., Sun, H., Zhou, J., et al. (2019). Denoising of 3d magnetic resonance images using a residual encoder–decoder wasserstein generative adversarial network. *Medical Image Analysis*, *55*, 165–180.

Remez, T., Litany, O., Giryes, R., & Bronstein, A. M. (2018). Class-aware fully convolutional Gaussian and Poisson denoising. *IEEE Transactions on Image Processing*, *27*(11), 5707–5722.

Ren, W., Liu, S., Ma, L., Xu, Q., Xu, X., Cao, X., et al. (2019). Low-light image enhancement via a deep hybrid network. *IEEE Transactions on Image Processing*, *28*(9), 4364–4375.

Ren, W., Pan, J., Zhang, H., Cao, X., & Yang, M.-H. (2020). Single image dehazing via multi-scale convolutional neural networks with holistic edges. *International Journal of Computer Vision*, *128*(1), 240–259.

Ren, D., Shang, W., Zhu, P., Hu, Q., Meng, D., & Zuo, W. (2020). Single image deraining using bilateral recurrent network. *IEEE Transactions on Image Processing*.

Ren, D., Zuo, W., Hu, Q., Zhu, P., & Meng, D. (2019). Progressive image deraining networks: a better and simpler baseline. In *Proceedings of the IEEE conference on computer vision and pattern recognition* (pp. 3937–3946).

Ren, D., Zuo, W., Zhang, D., Zhang, L., & Yang, M.-H. (2019). Simultaneous fidelity and regularization learning for image restoration. *IEEE Transactions on Pattern Analysis and Machine Intelligence*.

de Ridder, D., Duin, R. P., Verbeek, P. W., & Van Vliet, L. (1999). The applicability of neural networks to non-linear image processing. *Pattern Analysis & Applications*, *2*(2), 111–128.

Roth, S., & Black, M. J. (2005). Fields of experts: A framework for learning image priors. In *2005 IEEE computer society conference on computer vision and pattern recognition (CVPR'05), Vol. 2* (pp. 860–867). Citeseer.

Sadda, P., & Qarni, T. (2018). Real-time medical video denoising with deep learning: application to angiography. *International Journal of Applied Information Systems*, *12*(13), 22.

Schmidhuber, J. (2015). Deep learning in neural networks: An overview. *Neural Networks*, *61*, 85–117.

Schmidt, U., & Roth, S. (2014). Shrinkage fields for effective image restoration. In *Proceedings of the IEEE conference on computer vision and pattern recognition* (pp. 2774–2781).

Shantia, A., Timmers, R., Schomaker, L., & Wiering, M. (2015). Indoor localization by denoising autoencoders and semi-supervised learning in 3d simulated environment. In *2015 international joint conference on neural networks (IJCNN)* (pp. 1–7). IEEE.

Sheremet, O., Sheremet, K., Sadovoi, O., & Sokhina, Y. (2018). Convolutional neural networks for image denoising in infocommunication systems. In *2018 international scientific-practical conference problems of infocommunications. Science and technology (PIC S&T)* (pp. 429–432). IEEE.

Shwartz-Ziv, R., & Tishby, N. (2017). Opening the black box of deep neural networks via information. arXiv preprint arXiv:1703.00810.

Si, X., & Yuan, Y. (2018). Random noise attenuation based on residual learning of deep convolutional neural network. In *SEG technical program expanded abstracts 2018* (pp. 1986–1990). Society of Exploration Geophysicists.

Simonyan, K., & Zisserman, A. (2014). Very deep convolutional networks for large-scale image recognition. arXiv preprint arXiv:1409.1556.

Sivakumar, K., & Desai, U. B. (1993). Image restoration using a multilayer perceptron with a multilevel sigmoidal function. *IEEE Transactions on Signal Processing*, *41*(5), 2018–2022.

Soltanayev, S., & Chun, S. Y. (2018). Training deep learning based denoisers without ground truth data. In *Advances in neural information processing systems* (pp. 3257–3267).

Song, Y., Zhu, Y., & Du, X. (2019). Dynamic residual dense network for image denoising. *Sensors*, *19*(17), 3809.

Stone, J. E., Gohara, D., & Shi, G. (2010). Opencl: A parallel programming standard for heterogeneous computing systems. *Computing in Science & Engineering*, *12*(3), 66.

Su, Y., Lian, Q., Zhang, X., Shi, B., & Fan, X. (2019). Multi-scale cross-path concatenation residual network for Poisson denoising. *IET Image Processing*.

Sun, X., Kottayil, N. K., Mukherjee, S., & Cheng, I. (2018). Adversarial training for dual-stage image denoising enhanced with feature matching. In *International conference on smart multimedia* (pp. 357–366). Springer.

Szegedy, C., Liu, W., Jia, Y., Sermanet, P., Reed, S., Anguelov, D., et al. (2015). Going deeper with convolutions. In *Proceedings of the IEEE conference on computer vision and pattern recognition* (pp. 1–9).

Tai, Y., Yang, J., Liu, X., & Xu, C. (2017). Memnet: A persistent memory network for image restoration. In *Proceedings of the IEEE international conference on computer vision* (pp. 4539–4547).

Tamura, S. (1989). An analysis of a noise reduction neural network. In *International conference on acoustics, speech, and signal processing,* (pp. 2001–2004). IEEE.

Tan, H., Xiao, H., Lai, S., Liu, Y., & Zhang, M. (2019). Deep residual learning for burst denoising. In *2019 IEEE 4th international conference on image, vision and computing (ICIVC)* (pp. 156–161). IEEE.

Tao, L., Zhu, C., Song, J., Lu, T., Jia, H., & Xie, X. (2017). Low-light image enhancement using cnn and bright channel prior. In *2017 IEEE international conference on image processing (ICIP)* (pp. 3215–3219). IEEE.

Tao, L., Zhu, C., Xiang, G., Li, Y., Jia, H., & Xie, X. (2017). Llcnn: A convolutional neural network for low-light image enhancement. In *2017 IEEE visual communications and image processing (VCIP)* (pp. 1–4). IEEE.

Tassano, M., Delon, J., & Veit, T. (2019a). An analysis and implementation of the ffdnet image denoising method. *Image Processing On Line*, *9*, 1–25.

Tassano, M., Delon, J., & Veit, T. (2019b). Dvdnet: A fast network for deep video denoising. In *2019 IEEE International Conference on Image Processing (ICIP)* (pp. 1805–1809). IEEE.

Tian, C., Xu, Y., Fei, L., Wang, J., Wen, J., & Luo, N. (2019). Enhanced cnn for image denoising. *CAAI Transactions on Intelligence Technology*, *4*(1), 17–23.

Tian, C., Xu, Y., Fei, L., & Yan, K. (2018). Deep learning for image denoising: a survey. In *International conference on genetic and evolutionary computing* (pp. 563–572). Springer.

Tian, C., Xu, Y., Li, Z., Zuo, W., Fei, L., & Liu, H. (2020). Attention-guided cnn for image denoising. *Neural Networks*.

Tian, C., Xu, Y., & Zuo, W. (2020). Image denoising using deep cnn with batch renormalization. *Neural Networks*, *121*, 461–473.

Tian, C., Xu, Y., Zuo, W., Du, B., Lin, C.-W., & Zhang, D. (2020). Designing and training of a dual cnn for image denoising. arXiv preprint arXiv:2007.03951.

Tian, C., Xu, Y., Zuo, W., Zhang, B., Fei, L., & Lin, C.-W. (2020). Coarse-to-fine cnn for image super-resolution. *IEEE Transactions on Multimedia*.

Tian, C., Zhuge, R., Wu, Z., Xu, Y., Zuo, W., Chen, C., et al. (2020). Lightweight image super-resolution with enhanced cnn. *Knowledge-Based Systems*, 106235.

Tran, L., Yin, X., & Liu, X. (2017). Disentangled representation learning gan for pose-invariant face recognition. In *Proceedings of the IEEE conference on computer vision and pattern recognition* (pp. 1415–1424).

Tripathi, S., Lipton, Z. C., & Nguyen, T. Q. (2018). Correction by projection: Denoising images with generative adversarial networks. arXiv preprint arXiv:1803.04477.

Uchida, K., Tanaka, M., & Okutomi, M. (2018). Non-blind image restoration based on convolutional neural network. In *2018 IEEE 7th global conference on consumer electronics (GCCE)* (pp. 40–44). IEEE.

Vedaldi, A., & Lenc, K. (2015). Matconvnet: Convolutional neural networks for matlab. In *Proceedings of the 23rd ACM international conference on multimedia* (pp. 689–692). ACM.

Vogel, C., & Pock, T. (2017). A primal dual network for low-level vision problems. In *German conference on pattern recognition* (pp. 189–202). Springer.

Wang, X., Dai, F., Ma, Y., Guo, J., Zhao, Q., & Zhang, Y. (2019). Near-infrared image guided neural networks for color image denoising. In *ICASSP 2019-2019 IEEE international conference on acoustics, speech and signal processing (ICASSP)* (pp. 3807–3811). IEEE.

Wang, T., Qin, Z., & Zhu, M. (2017). An ELU network with total variation for image denoising. In *International conference on neural information processing* (pp. 227–237). Springer.

Wang, T., Sun, M., & Hu, K. (2017). Dilated deep residual network for image denoising. In *2017 IEEE 29th international conference on tools with artificial intelligence (ICTAI)* (pp. 1272–1279). IEEE.

Wang, H., Wang, Q., Gao, M., Li, P., & Zuo, W. (2018). Multi-scale location-aware kernel representation for object detection. In *Proceedings of the IEEE conference on computer vision and pattern recognition* (pp. 1248–1257).

Wang, C., Zhou, S. K., & Cheng, Z. (2020). First image then video: A two-stage network for spatiotemporal video denoising. arXiv preprint arXiv:2001.00346.

Wei, J., Xia, Y., & Zhang, Y. (2019). M3net: A multi-model, multi-size, and multi-view deep neural network for brain magnetic resonance image segmentation. *Pattern Recognition*, *91*, 366–378.

Wen, J., Xu, Y., & Liu, H. (2020). Incomplete multiview spectral clustering with adaptive graph learning. *IEEE Transactions on Cybernetics*, *50*(4), 1418–1429.

Wen, J., Zhang, Z., Zhang, Z., Fei, L., & Wang, M. (2020). Generalized incomplete multiview clustering with flexible locality structure diffusion. *IEEE Transactions on Cybernetics*.

Wu, D., Ren, H., & Li, Q. (2020). Self-supervised dynamic ct perfusion image denoising with deep neural networks. arXiv preprint arXiv:2005.09766.

Wu, S., & Xu, Y. (2019). Dsn: A new deformable subnetwork for object detection. *IEEE Transactions on Circuits and Systems for Video Technology*.

Xia, Z., Perazzi, F., Gharbi, M., Sunkavalli, K., & Chakrabarti, A. (2019). Basis prediction networks for effective burst denoising with large kernels. arXiv preprint arXiv:1912.04421.

Xiao, P., Guo, Y., & Zhuang, P. (2018). Removing stripe noise from infrared cloud images via deep convolutional networks. *IEEE Photonics Journal*, *10*(4), 1–14.

Xiao, X., Xiong, N. N., Lai, J., Wang, C.-D., Sun, Z., & Yan, J. (2019). A local consensus index scheme for random-valued impulse noise detection systems. *IEEE Transactions on Systems, Man, and Cybernetics: Systems*.

Xie, W., Li, Y., & Jia, X. (2018). Deep convolutional networks with residual learning for accurate spectral-spatial denoising. *Neurocomputing*, *312*, 372–381.

Xu, J., Li, H., Liang, Z., Zhang, D., & Zhang, L. (2018). Real-world noisy image denoising: A new benchmark. arXiv preprint arXiv:1804.02603.

Xu, X., Li, M., & Sun, W. (2019). Learning deformable kernels for image and video denoising. arXiv preprint arXiv:1904.06903.

Xu, Q., Zhang, C., & Zhang, L. (2015). Denoising convolutional neural network. In *2015 IEEE international conference on information and automation* (pp. 1184–1187). IEEE.

Xu, J., Zhang, L., & Zhang, D. (2018b). A trilateral weighted sparse coding scheme for real-world image denoising. In *Proceedings of the European conference on computer vision (ECCV)* (pp. 20–36).

Xu, J., Zhang, L., & Zhang, D. (2018c). External prior guided internal prior learning for real-world noisy image denoising. *IEEE Transactions on Image Processing*, *27*(6), 2996–3010.

Xu, J., Zhang, L., Zuo, W., Zhang, D., & Feng, X. (2015). Patch group based nonlocal self-similarity prior learning for image denoising. In *Proceedings of the IEEE international conference on computer vision* (pp. 244–252).

Yan, H., Tan, V., Yang, W., & Feng, J. (2019). Unsupervised image noise modeling with self-consistent gan. arXiv preprint arXiv:1906.05762.

Yang, J., Chu, D., Zhang, L., Xu, Y., & Yang, J. (2013). Sparse representation classifier steered discriminative projection with applications to face recognition. *IEEE Transactions on Neural Networks and Learning Systems*, *24*(7), 1023–1035.

Yang, J., Liu, X., Song, X., & Li, K. (2017). Estimation of signal-dependent noise level function using multi-column convolutional neural network. In *2017 IEEE international conference on image processing (ICIP)* (pp. 2418–2422). IEEE.

Yang, D., & Sun, J. (2017). Bm3d-net: A convolutional neural network for transform-domain collaborative filtering. *IEEE Signal Processing Letters*, *25*(1), 55–59.

Yang, J., Zhang, L., Xu, Y., & Yang, J.-y. (2012). Beyond sparsity: The role of l1-optimizer in pattern classification. *Pattern Recognition*, *45*(3), 1104–1118.

Yao, Y., Wu, X., Zhang, L., Shan, S., & Zuo, W. (2018). Joint representation and truncated inference learning for correlation filter based tracking. In *Proceedings of the European conference on computer vision (ECCV)* (pp. 552–567).

Ye, J. C., Han, Y., & Cha, E. (2018). Deep convolutional framelets: A general deep learning framework for inverse problems. *SIAM Journal on Imaging Sciences*, *11*(2), 991–1048.

Yeh, R. A., Lim, T. Y., Chen, C., Schwing, A. G., Hasegawa-Johnson, M., & Do, M. (2018). Image restoration with deep generative models. In *2018 IEEE international conference on acoustics, speech and signal processing (ICASSP)* (pp. 6772–6776). IEEE.

Yi, D., Lei, Z., Liao, S., & Li, S. Z. (2014). Learning face representation from scratch. arXiv preprint arXiv:1411.7923.

Yu, A., Liu, X., Wei, X., Fu, T., & Liu, D. (2018). Generative adversarial networks with dense connection for optical coherence tomography images denoising. In *2018 11th international congress on image and signal processing, biomedical engineering and informatics (CISP-BMEI)* (pp. 1–5). IEEE.

Yu, S., Ma, J., & Wang, W. (2019). Deep learning for denoising. *Geophysics*, *84*(6), V333–V350.

Yuan, D., Fan, N., & He, Z. (2020). Learning target-focusing convolutional regression model for visual object tracking. *Knowledge-Based Systems*, Article 105526.

Yuan, D., Li, X., He, Z., Liu, Q., & Lu, S. (2020). Visual object tracking with adaptive structural convolutional network. *Knowledge-Based Systems*, Article 105554.

Yuan, Y., Liu, S., Zhang, J., Zhang, Y., Dong, C., & Lin, L. (2018). Unsupervised image super-resolution using cycle-in-cycle generative adversarial networks. In *Proceedings of the IEEE conference on computer vision and pattern recognition workshops* (pp. 701–710).

Yuan, Q., Zhang, Q., Li, J., Shen, H., & Zhang, L. (2018). Hyperspectral image denoising employing a spatial–spectral deep residual convolutional neural network. *IEEE Transactions on Geoscience and Remote Sensing*, *57*(2), 1205–1218.

Yue, Z., Yong, H., Zhao, Q., Meng, D., & Zhang, L. (2019). Variational denoising network: Toward blind noise modeling and removal. In *Advances in neural information processing systems* (pp. 1688–1699).

Zamparelli, M. (1997). Genetically trained cellular neural networks. *Neural Networks*, *10*(6), 1143–1151.

Zarshenas, A., & Suzuki, K. (2018). Deep neural network convolution for natural image denoising. In *2018 IEEE international conference on systems, man, and cybernetics (SMC)* (pp. 2534–2539). IEEE.

Zha, Z., Yuan, X., Yue, T., & Zhou, J. (2018). From rank estimation to rank approximation: Rank residual constraint for image denoising. arXiv preprint arXiv:1807.02504.

Zhang, Z., Geiger, J., Pohjalainen, J., Mousa, A. E.-D., Jin, W., & Schuller, B. (2018). Deep learning for environmentally robust speech recognition: An overview of recent developments. *ACM Transactions on Intelligent Systems and Technology (TIST)*, *9*(5), 49.

Zhang, J., & Ghanem, B. (2018). ISTA-Net: Interpretable optimization-inspired deep network for image compressive sensing. In *Proceedings of the IEEE conference on computer vision and pattern recognition* (pp. 1828–1837).

Zhang, B., Jin, S., Xia, Y., Huang, Y., & Xiong, Z. (2020). Attention mechanism enhanced kernel prediction networks for denoising of burst images. In *ICASSP 2020-2020 IEEE international conference on acoustics, speech and signal processing (ICASSP)* (pp. 2083–2087). IEEE.

Zhang, F., Liu, D., Wang, X., Chen, W., & Wang, W. (2018). Random noise attenuation method for seismic data based on deep residual networks. In *International geophysical conference, Beijing, China, 24-27 April 2018* (pp. 1774–1777). Society of Exploration Geophysicists and Chinese Petroleum Society.

Zhang, Z., Wang, L., Kai, A., Yamada, T., Li, W., & Iwahashi, M. (2015). Deep neural network-based bottleneck feature and denoising autoencoder-based dereverberation for distant-talking speaker identification. *EURASIP Journal on Audio, Speech, and Music Processing*, *2015*(1), 12.

Zhang, L., Wu, X., Buades, A., & Li, X. (2011). Color demosaicking by local directional interpolation and nonlocal adaptive thresholding. *Journal of Electronic imaging*, *20*(2), Article 023016.

Zhang, M., Zhang, F., Liu, Q., & Wang, S. (2019). Vst-net: Variance-stabilizing transformation inspired network for Poisson denoising. *Journal of Visual Communication and Image Representation*, *62*, 12–22.

Zhang, L., Zhang, L., Mou, X., & Zhang, D. (2011). Fsim: A feature similarity index for image quality assessment. *IEEE Transactions on Image Processing*, *20*(8), 2378–2386.

Zhang, L., & Zuo, W. (2017). Image restoration: From sparse and low-rank priors to deep priors [lecture notes]. *IEEE Signal Processing Magazine*, *34*(5), 172–179.

Zhang, K., Zuo, W., Chen, Y., Meng, D., & Zhang, L. (2017). Beyond a gaussian denoiser: Residual learning of deep cnn for image denoising. *IEEE Transactions on Image Processing*, *26*(7), 3142–3155.

Zhang, K., Zuo, W., Gu, S., & Zhang, L. (2017). Learning deep cnn denoiser prior for image restoration. In *Proceedings of the IEEE conference on computer vision and pattern recognition* (pp. 3929–3938).

Zhang, K., Zuo, W., & Zhang, L. (2018a). Ffdnet: Toward a fast and flexible solution for cnn-based image denoising. *IEEE Transactions on Image Processing*, *27*(9), 4608–4622.

Zhang, K., Zuo, W., & Zhang, L. (2018b). Learning a single convolutional super-resolution network for multiple degradations. In *Proceedings of the IEEE conference on computer vision and pattern recognition* (pp. 3262–3271).

Zhang, K., Zuo, W., & Zhang, L. (2019). Deep plug-and-play super-resolution for arbitrary blur kernels. In *Proceedings of the IEEE conference on computer vision and pattern recognition* (pp. 1671–1681).

Zhao, D., Ma, L., Li, S., & Yu, D. (2019). End-to-end denoising of dark burst images using recurrent fully convolutional networks. arXiv preprint arXiv:1904.07483.

Zhao, H., Shao, W., Bao, B., & Li, H. (2019). A simple and robust deep convolutional approach to blind image denoising. In *Proceedings of the IEEE international conference on computer vision workshops* (pp. 0-0).

Zheng, Y., Duan, H., Tang, X., Wang, C., & Zhou, J. (2019). Denoising in the dark: Privacy-preserving deep neural network based image denoising. *IEEE Transactions on Dependable and Secure Computing*.

ZhiPing, Q., YuanQi, Z., Yi, S., & XiangBo, L. (2018). A new generative adversarial network for texture preserving image denoising. In *2018 eighth international conference on image processing theory, tools and applications (IPTA)* (pp. 1–5). IEEE.

Zhou, Y., Chellappa, R., & Jenkins, B. (1987). A novel approach to image restoration based on a neural network. In *Proceedings of the international conference on neural networks*, San Diego, California.

Zoran, D., & Weiss, Y. (2011). From learning models of natural image patches to whole image restoration. In *2011 international conference on computer vision* (pp. 479–486). IEEE.

Zuo, W., Zhang, L., Song, C., Zhang, D., & Gao, H. (2014). Gradient histogram estimation and preservation for texture enhanced image denoising. *IEEE Transactions on Image Processing*, *23*(6), 2459–2472.